



**HAL**  
open science

## Synthesis and antimicrobial testing of 5-fluorouracil derivatives

Mrunal Patil, Krykun Serhii, Frédéric Garzino, Quentin Gobert, Suzanne Giorgio, Jean-manuel Raimundo, Jean-michel Bolla, Michel Camplo

► **To cite this version:**

Mrunal Patil, Krykun Serhii, Frédéric Garzino, Quentin Gobert, Suzanne Giorgio, et al.. Synthesis and antimicrobial testing of 5-fluorouracil derivatives. *Archiv der Pharmazie / Chemistry in Life Sciences*, 2023, 356 (7), 10.1002/ardp.202300103 . hal-04434598

**HAL Id: hal-04434598**

**<https://hal.science/hal-04434598>**

Submitted on 2 Feb 2024




**HAL** is a multi-disciplinary open access archive for the deposit and dissemination of scientific research documents, whether they are published or not. The documents may come from teaching and research institutions in France or abroad, or from public or private research centers.

L'archive ouverte pluridisciplinaire **HAL**, est destinée au dépôt et à la diffusion de documents scientifiques de niveau recherche, publiés ou non, émanant des établissements d'enseignement et de recherche français ou étrangers, des laboratoires publics ou privés.



Distributed under a Creative Commons Attribution 4.0 International License

# Synthesis and antimicrobial testing of 5-fluorouracil derivatives

Mrunal Patil<sup>1</sup> | Krykun Serhii<sup>2</sup>  | Frédéric Garzino<sup>2</sup> | Quentin Gobert<sup>2</sup> |  
Suzanne Giorgio<sup>2</sup>  | Jean-Manuel Raimundo<sup>2</sup> | Jean-Michel Bolla<sup>1</sup> |  
Michel Camplo<sup>2</sup> 

<sup>1</sup>Aix Marseille Université, INSERM, SSA, MCT, Marseille, France

<sup>2</sup>Aix Marseille Université, CNRS, CINaM UMR 7325, Campus de Luminy, Marseille, France

## Correspondence

Jean-Michel Bolla, Aix Marseille Université, INSERM, SSA, MCT, 13385 Marseille, France.  
Email: [Jean-michel.BOLLA@univ-amu.fr](mailto:Jean-michel.BOLLA@univ-amu.fr)

Michel Camplo, Aix Marseille Université, CNRS, CINaM UMR 7325, Campus de Luminy, Case 913, 13288 Marseille Cedex 09, France.  
Email: [michel.camplo@univ-amu.fr](mailto:michel.camplo@univ-amu.fr)

## Funding information

Amidex Foundation, A-M-AAPID-17-22-170228-18.54; Inserm, CNRS, MESRI

## Abstract

Antibiotic resistance has increased the demand for novel treatments against multidrug-resistant microorganisms. In the research literature, 5-fluorouracil (5-FU) was proposed as an alternative due to its intrinsic antibacterial property. However, given its toxicity profile at high doses, its use in antibacterial therapy is dubious. In the quest for improving the efficacy of 5-FU, the present study intends to synthesise 5-FU derivatives and assess their susceptibility and mechanism against pathogenic bacteria. It was found that the compounds having tri-hexylphosphonium substitution on both nitrogen groups of 5-FU (**6a**, **6b** and **6c**) had considerable activity against both Gram-positive and Gram-negative bacteria. Among the active compounds, those with an asymmetric linker group **6c** were found to have higher antibacterial efficacy. However, no conclusive efflux inhibition activity was found. As elucidated by electron microscopy studies, these self-assembling active phosphonium-based 5-FU derivatives caused considerable septal damage and cytosolic alterations in *Staphylococcus aureus* cells. In *Escherichia coli*, these compounds triggered plasmolysis. Interestingly, the minimal inhibitory concentration (MIC) of the most potent 5-FU derivative **6c** remained constant, regardless of the bacteria's resistance profile. Further analysis revealed that compound **6c** generated significant alterations in membrane permeabilization and depolarization in *S. aureus* and *E. coli* cells at the MIC. Compound **6c** was found to substantially impede bacterial motility, suggesting its importance in regulating bacterial pathogenicity. Additionally, the nonhaemolytic activity of **6c** suggested that it could be a potential therapeutic option for treating multidrug-resistant bacterial infections.

## KEYWORDS

5-fluorouracil, antimicrobial, microscopy, phosphonium derivatives

This is an open access article under the terms of the Creative Commons Attribution-NonCommercial-NoDerivs License, which permits use and distribution in any medium, provided the original work is properly cited, the use is non-commercial and no modifications or adaptations are made.

© 2023 The Authors. *Archiv der Pharmazie* published by Wiley-VCH GmbH on behalf of Deutsche Pharmazeutische Gesellschaft.

## 1 | INTRODUCTION

Exhaustive use and misuse of antibiotics in humans, animals and agriculture have accelerated the crisis of resistance in bacteria.<sup>[1]</sup> Resistance develops genetically, either through mutation or by the acquisition of new resistance genes via genetic exchange mechanisms. The incidence of multidrug-resistant (MDR) bacteria, predominantly those from the ESKAPE group (ESKAPE is an acronym for the scientific names of six highly virulent and antibiotic-resistant bacterial pathogens: *Enterococcus faecium*, *Staphylococcus aureus*, *Klebsiella pneumoniae*, *Acinetobacter baumannii*, *Pseudomonas aeruginosa* and *Enterobacter* spp.), are increasing morbidity and mortality rates all across the world.<sup>[2]</sup> It is anticipated that if no solution is found, roughly 10 million people will die by 2050, surpassing cancer deaths.<sup>[3]</sup> Every year, 23,000 patients die in developed countries such as the United States due to a lack of treatment alternatives for MDR patients.<sup>[4]</sup> The situation in developing countries like India is more dire, wherein more than 58,000 infants died in 2013 as a result of antibiotic-resistant bacteria infections.<sup>[5]</sup> It's also crucial to note that there haven't been many new antibiotic breakthroughs to tackle bacteria that are resistant to antibiotics. One of the reasons could be that pharmaceutical companies are no longer effectively investing in the discovery of novel antibiotics in comparison to drugs for chronic diseases. Due to this, clinicians frequently opt for combination treatment regimens, which necessitate extended hospitalisation and much more resource expenditure (ICU and monitoring).<sup>[6,7]</sup> This situation has led to significant economic consequences, causing monetary losses for both individuals and governments. According to different studies, it is projected that antimicrobial resistance (AMR) could cost from \$300 billion to more than \$1 trillion annually by 2050 worldwide.<sup>[8,9]</sup> In the quest to combat this issue, researchers have recommended drug repurposing. Drug repurposing is a method that is applied to identify novel therapeutic agents from clinically approved drug molecules.<sup>[10]</sup> For example, recently, antiviral drugs like remdesivir and favipiravir have been repositioned for the treatment of COVID-19.<sup>[11]</sup> It is regarded as an effective method for developing drug candidates with novel therapeutic or pharmacological characteristics. This approach has many advantages over the conventional drug discovery procedure, including a reduced drug development timeline, lower costs, higher efficiency and a lower risk of failure.

One such drug is 5-fluorouracil (5-FU), arguably the most successful chemotherapeutic agent.<sup>[12]</sup> However, its potential as an antibacterial agent has not been thoroughly investigated. Cohen et al.<sup>[13]</sup> were the first to investigate the antimicrobial effect of 5-FU in *Escherichia coli*. They found that 5-FU caused 'thymineless death' in bacteria by inhibiting the enzyme thymidylate synthase, which is required for DNA synthesis. In another investigation, 5-FU-treated *E. coli* K-12 cells were found to be more susceptible to heat and mechanical stress due to osmotic imbalance produced by cell wall precursor accumulation.<sup>[14]</sup> In addition, the biofilm and virulence inhibition activities of 5-FU are also well documented. 5-FU acts as a potent quorum-quencher, inhibiting quorum-sensor autoinducer-2

production released by methicillin-resistant *S. aureus* (MRSA), *Staphylococcus epidermidis*, *E. coli* and *Vibrio harveyi*.<sup>[15]</sup> In addition, Ueda et al. demonstrated the nontoxicity of 5-FU and its ability to prevent the growth of biofilms in *P. aeruginosa*. Their results were found to be consistent with those obtained by Hussain et al. on the biofilm formation of *S. epidermidis*.<sup>[16,17]</sup> Given its antivirulence properties, 5-FU is unlikely to develop resistance. However, because 5-FU is a BCS class III drug, its permeability is low, restricting its drug delivery.<sup>[18]</sup> Furthermore, it is said to have had a significant level of cardiotoxicity and a short half-life. Most importantly, drugs such as ceftazidime (CFT) and cefepime (CFP) have been shown to interfere with the action of 5-FU.<sup>[19]</sup> As a result, it is critical to investigate 5-FU derivatives to overcome the aforementioned issues.

Previously, our research team developed and evaluated phosphonium compounds with antibacterial activity comparable to commercially used antibiotics. These amphiphilic phosphonium derivatives could self-organize into vesicles of varying sizes, making them potential nano-drug delivery tools.<sup>[20-23]</sup> Additionally, it has been suggested that nano-sized assemblies might help to enhance biological activities.<sup>[24]</sup> Considering the aforementioned, the authors of this paper were intrigued to investigate the antibacterial properties of 5-FU-based phosphonium derivatives. In this article, six 5-FU-based mono- and di-substituted derivatives bearing phosphonium side chains linked with a (C4-C10) spacer were synthesised and evaluated for their physicochemical properties and antibacterial activity against ESKAPE group bacteria.

## 2 | RESULTS AND DISCUSSION

### 2.1 | Chemistry

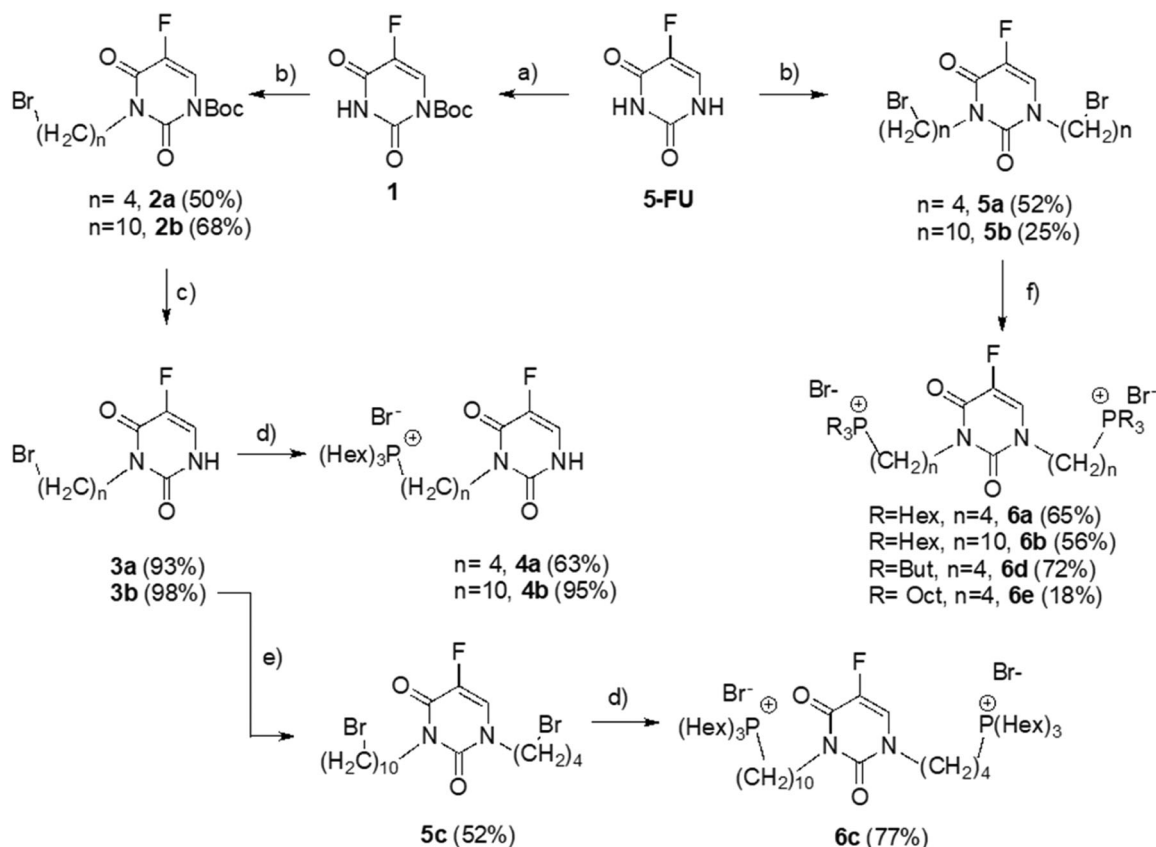
Details of the synthesis of each molecule, yield and characterization are discussed in Supporting Information: Section S1 and structures of respective 5-FU derivatives are illustrated in Supporting Information: Figures S1-S15. The reaction scheme is given in Scheme 1.

### 2.2 | Susceptibility assay

Table 1 summarizes the bacterial strains utilized in the current and subsequent studies.

#### 2.2.1 | Susceptibility assay on ESKAPE group bacteria

The minimal inhibitory concentration (MIC) values of 5-FU and its derivatives against reference ESKAPE strains are specified in Table 2. It is well known that 5-FU exhibits some inherent antibacterial activity.<sup>[15]</sup> As tested, we found that 5-FU showed considerable activity against Gram-positive bacteria like *S. aureus* (2 µg/mL) and *E. faecium* (4 µg/mL) and some of the Gram-negative bacteria like



**SCHEME 1** Scheme for the synthesis of 5-FU derivatives. Reagents and conditions: (a) Boc<sub>2</sub>O, 4-DMAP, CH<sub>3</sub>CN, R.T.; (b) NaH, DMF, R.T.; then Br-(CH<sub>2</sub>)<sub>n</sub>-Br; (c) K<sub>2</sub>CO<sub>3</sub>, MeOH, R.T.; (d) P(Hex)<sub>3</sub>, CH<sub>3</sub>CN, microwaves, 85°C; (e) NaH, DMF, R.T., then Br-(CH<sub>2</sub>)<sub>4</sub>-Br; (f) PR<sub>3</sub>, CH<sub>3</sub>CN, microwaves, 200 W, 85°C.

*K. pneumoniae* (4 µg/mL) and *E. coli* (16 µg/mL). However, its activity against other bacteria such as *P. aeruginosa*, *Enterobacter aerogenes* and *A. baumannii* was found to be poor ( $\geq 64$  g/mL). When 5-FU derivatives were tested against ESKAPE strains, only those with tri-hexylphosphonium substitution (**4a**, **4b**, **6a**, **6b**, **6c**) showed activity against Gram-positive bacteria. Interestingly, it was observed that among these, the compounds that had tri-hexylphosphonium substituted on both the nitrogen of 5-FU structure (**6a**, **6b**, **6c**) exhibited activity against Gram-negative bacteria too. Additionally, compounds having non-tri-hexylphosphonium side chains, such as **6d** (containing tri-butylphosphonium) and **6e** (containing tri-octylphosphonium), were found to be inactive against both Gram-positive and Gram-negative bacteria. This highlights the importance of tri-hexylphosphonium substitution on both nitrogen groups of 5-FU to produce an effect in both Gram-negative and Gram-positive bacteria. As observed, the potencies of these active compounds (**6c** > **6a** > **6b**) varied according to the chain length of the spacer alkyl group (Figure 1). The most active molecule (**6c**) had an asymmetric structure with C4 and C10 alkyl spacer chains on either nitrogen group of the 5-FU structure. However, compounds **6a** and **6b** had symmetric spacer alkyl chains C4 and C10 linked to their nitrogen groups, respectively. We believe that the presence of the C10 alkyl chain might have imparted higher hydrophobicity to compound **6b**,

thereby causing a decrease in its inhibition activity. In addition, although **6c** was the most active derivative, its MIC against *K. pneumoniae* was not different from that of 5-FU. The same was true for the tested Gram-positive bacteria, *S. aureus* and *E. faecium*.

## 2.2.2 | Susceptibility assay on efflux mutants

To ascertain whether any of these substances were possible efflux pump substrates, they were tested against Gram-positive and Gram-negative bacterial efflux mutants (details of mutants given in Table 1). Table 3 shows that in the case of *S. aureus* *norA* efflux mutants and *E. aerogenes* *acrAB-tolC* efflux mutants, regardless of efflux gene deletion or overexpression, none of the compounds showed a significant variation in their MIC values. Compounds with MIC values >512 g/mL were excluded because they precipitated or became turbid at higher concentrations. As a result, the obtained results seem to be unreliable. Having said that, it could be concluded that none of the derivatives had substrate specificity for the *S. aureus* *norA* efflux pump or the *E. aerogenes* *acrAB-TolC* efflux pump. However, compounds **4a**, **4b** and **6d** depicted differential MIC among wild-type and *acrAB*-deleted strains of *E. coli*. Therefore, to reaffirm their effect, these compounds were evaluated in combination with

**TABLE 1** List of bacteria used in the present study.

Strain	Source	Relevant features	References
<i>Reference bacteria</i>			
ATCC 13048	American-type culture collection	<i>Enterobacter aerogenes</i>	[20]
ATCC 19434		<i>Enterococcus faecium</i>	
ATCC 25923		<i>Staphylococcus aureus</i>	
ATCC 11775		<i>Escherichia coli</i>	
ATCC 13883		<i>Klebsiella pneumoniae</i>	
ATCC 19606		<i>Acinetobacter baumannii</i>	
ATCC 10145		<i>Pseudomonas aeruginosa</i>	
<i>S. aureus</i>			
SA1199	Endocarditis patient	Clinical isolate, methicillin susceptible	[25, 26]
SA1199B	Derivative of SA1199	<i>norA</i> -overproducing derivative of SA-1199; also has A116E GrlA substitution	
SAK1758	Derivative of NCTC-8325-4	Knocked out NorA ( $\Delta norA$ )	
SA 1	Urine	Clinical isolates from HIA-Laveran, Marseille: CHL <sup>r</sup> , NAL*	This study
SA 2	Sputum	Clinical isolates from HIA-Laveran, Marseille: OFL <sup>r</sup> , CFX <sup>r</sup> , CIP <sup>r</sup> , CHL <sup>r</sup> , NOR*, NAL*	
SA 3	Sputum	Clinical isolates from HIA-Laveran, Marseille: OFL <sup>r</sup> , CLN <sup>r</sup> , CHL <sup>r</sup> , ERY <sup>r</sup> , CIP <sup>r</sup> , NOR*, NAL*	
SA 9	Sputum	Clinical isolates from HIA-Laveran, Marseille: OFL <sup>r</sup> , CLN <sup>r</sup> , NEO <sup>r</sup> , CFX <sup>r</sup> , CIP <sup>r</sup> , CHL <sup>r</sup> , ERY <sup>r</sup> , NOR*, NAL*	
SA 11	Skin	Clinical isolates from HIA-Laveran, Marseille: OFL <sup>r</sup> , CLN <sup>r</sup> , CIP <sup>r</sup> , CHL <sup>r</sup> , ERY <sup>r</sup> , NOR*, NAL*	
SA 12	Skin	Clinical isolates from HIA-Laveran, Marseille: CHL <sup>r</sup> , ERY <sup>r</sup> , NAL*	
<i>E. aerogenes</i>			
EA27	Urinary tract	MDR clinical isolate; KAN <sup>r</sup> AMP <sup>r</sup> CHL <sup>r</sup> NAL <sup>r</sup> STR <sup>r</sup> TET <sup>r</sup> ( <b>acrA+</b> , <b>ToIC+</b> )	[27]
EA289	Derivative of EA-27	KAN-sensitive ( <b>acrA+</b> , <b>ToIC+</b> )	
EA294	Derivative of EA289	$\Delta acrA$ :: KAN <sup>r</sup> ( <b>acrA-</b> , <b>ToIC+</b> )	
<i>E. coli</i>			
AG100	Derivative of K-12 strain	Wild-type <i>E. coli</i> K-12 ( <b>acrAB+</b> , <b>ToIC+</b> )	[27, 28]
AG100A	Derivative of AG100	<i>AcrAB</i> deleted, $\Delta acrAB$ :: KAN <sup>r</sup> ( <b>acrAB-</b> , <b>ToIC+</b> )	
AG102	Derivative of AG100	Overexpressing <i>AcrAB</i> pump ( <b>acrAB++</b> , <b>ToIC+</b> )	
AG100A <sub>TET</sub>	Derivative of AG100A	TET <sup>r</sup> derivative of AG100A in which the <i>acrF</i> gene is markedly overexpressed	
T-AG100	Derivative of AG100 strain	<i>E. coli</i> AG100 transformed with pACYC184-ampRC	This study
EC-LAV-1	Urine	Clinical isolates from HIA-Laveran, Marseille: NOR <sup>r</sup> , NAL <sup>r</sup> , ZDM <sup>r</sup> , AMP <sup>r</sup> , AMK <sup>r</sup> , ERY*	
EC-LAV-3	Urine	Clinical isolates from HIA-Laveran, Marseille: ERY*	
EC-LAV-4	Urine	Clinical isolates from HIA-Laveran, Marseille: ERY*	
EC-LAV-7	Faecal matter	Clinical isolates from HIA-Laveran, Marseille: GEN <sup>r</sup> , CIP <sup>r</sup> , NOR <sup>r</sup> , NAL <sup>r</sup> , CHL <sup>r</sup> , TET <sup>r</sup> , TOB <sup>r</sup> , CTX <sup>r</sup> , ZDM <sup>r</sup> , AMP <sup>r</sup> , AMK <sup>r</sup> , MERO <sup>r</sup> , ERY*, DOX*	
EC-LAV-8	Urine	Clinical isolates from HIA-Laveran, Marseille: GEN <sup>r</sup> , CIP <sup>r</sup> , NOR <sup>r</sup> , TET <sup>r</sup> , TOB <sup>r</sup> , CTX <sup>r</sup> , ZDM <sup>r</sup> , AMP <sup>r</sup> , ERY*, DOX*	
EC-LAV-11	Urine	Clinical isolates from HIA-Laveran, Marseille: CTX <sup>r</sup> , ZDM <sup>r</sup> , AMP <sup>r</sup> , ERY*	
<i>P. aeruginosa</i>			
PAO1	Infected wound	Reference strain	[29, 30]
PA402	Derivative of PAO1	<i>mex AB</i> deleted ( $\Delta mex AB$ )	
$\Delta MEX D$		<i>mex D</i> deleted ( $\Delta mex D$ )	[31]
$\Delta MEX F$		<i>mex F</i> deleted ( $\Delta mex F$ )	

TABLE 1 (Continued)

Strain	Source	Relevant features	References
PA403		Efflux pump deleted ( $\Delta$ mex AB, $\Delta$ mex CD, $\Delta$ mex EF, $\Delta$ mex XY, $\Delta$ mex JK)	[32]
PT629		mex AB overexpressing (mex AB++)	[33]
PA01 ERY <sup>R</sup>		mex CD overexpressing (mex CD++)	
PA0-7H		mex EF overexpressing (mex EF++)	
CMZ091		mex XY overexpressing (mex XY++)	
PA2013-LAV-1	Superficial pus	Clinical isolates from HIA-Laveran, Marseille: ZDM <sup>r</sup> , PIP <sup>r</sup> , NAL <sup>*</sup> , CHL <sup>*</sup> , ERY <sup>*</sup> , TET <sup>*</sup> , DOX <sup>*</sup>	
PA2013-LAV-2	Urine	Clinical isolates from HIA-Laveran, Marseille: ZDM <sup>r</sup> , PIP <sup>r</sup> , NAL <sup>*</sup> , CHL <sup>*</sup> , ERY <sup>*</sup> , TET <sup>*</sup> , DOX <sup>*</sup>	
PA2013-LAV-3	Urine	Clinical isolates from HIA-Laveran, Marseille: GEN <sup>r</sup> , CIP <sup>r</sup> , TOB <sup>r</sup> , AMK <sup>r</sup> , PIP <sup>r</sup> , IMI <sup>r</sup> , MERO <sup>r</sup> , NAL <sup>*</sup> , CHL <sup>*</sup> , ERY <sup>*</sup> , TET <sup>*</sup> , DOX <sup>*</sup>	
PA2013-LAV-5	Lung	Clinical isolates from HIA-Laveran, Marseille: GEN <sup>r</sup> , CIP <sup>r</sup> , TOB <sup>r</sup> , ZDM <sup>r</sup> , DOX <sup>r</sup> , AMK <sup>r</sup> , PIP <sup>r</sup> , IMI <sup>r</sup> , MERO <sup>r</sup> , NAL <sup>*</sup> , CHL <sup>*</sup> , ERY <sup>*</sup> , TET <sup>*</sup> , DOX <sup>*</sup>	
PA2013-LAV-14	Urine	Clinical isolates from HIA-Laveran, Marseille: GEN <sup>r</sup> , CIP <sup>r</sup> , TOB <sup>r</sup> , AMK <sup>r</sup> , PIP <sup>r</sup> , NAL <sup>*</sup> , CHL <sup>*</sup> , ERY <sup>*</sup> , TET <sup>*</sup> , DOX <sup>*</sup>	
PA2013-LAV-17	Drainage fluid	Clinical isolates from HIA-Laveran, Marseille: ZDM <sup>r</sup> , PIP <sup>r</sup> , MERO <sup>r</sup> , NAL <sup>*</sup> , CHL <sup>*</sup> , ERY <sup>*</sup> , TET <sup>*</sup> , DOX <sup>*</sup>	
<i>K. pneumoniae</i>			
KPBJ 2	Blood	Clinical isolates from Beaujon hospital, Paris: NAL <sup>*</sup> , CHL <sup>*</sup> , ERY <sup>*</sup> , PIP <sup>*</sup>	[34]
KPBJ 4	Blood	Clinical isolates from Beaujon hospital, Paris: MERO <sup>r</sup> , NAL <sup>*</sup> , CHL <sup>*</sup> , ERY <sup>*</sup>	
KPBJ 6	Hepatic drainage fluid	Clinical isolates from Beaujon hospital, Paris: CIP <sup>r</sup> , CFX <sup>r</sup> , MERO <sup>r</sup> , NOR <sup>*</sup> , NAL <sup>*</sup> , CHL <sup>*</sup> , ERY <sup>*</sup> , PIP <sup>*</sup>	
KPBJ 7	Blood	Clinical isolates from Beaujon hospital, Paris: CFX <sup>r</sup> , OFL <sup>*</sup> , NAL <sup>*</sup> , CHL <sup>*</sup> , ERY <sup>*</sup> , TET <sup>*</sup> , DOX <sup>*</sup> , PIP <sup>*</sup>	
KPBJ 11	Blood	Clinical isolates from Beaujon hospital, Paris: NAL <sup>*</sup> , CHL <sup>*</sup> , ERY <sup>*</sup> , PIP <sup>*</sup>	
KP55	Sputum	Clinical isolates from Beaujon hospital, Paris: GEN <sup>r</sup> , TOB <sup>r</sup> , CFX <sup>r</sup> , CTX <sup>r</sup> , ZDM <sup>r</sup> , COL <sup>r</sup> , AMK <sup>r</sup> , PIP <sup>r</sup> , IMI <sup>r</sup> , MERO <sup>r</sup> , OFL <sup>*</sup> , NAL <sup>*</sup> , CHL <sup>*</sup> , ERY <sup>*</sup> , TET <sup>*</sup> , DOX <sup>*</sup>	[27, 35]
<i>A. baumannii</i>			
AB866	QC for VITEK <sup>®</sup> analysis	CIP <sup>r</sup> , TET <sup>r</sup> , TOB <sup>r</sup> , CTX <sup>r</sup> , ZDM <sup>r</sup> , DOX <sup>r</sup> , AMK <sup>r</sup> , MERO <sup>r</sup> , NOR <sup>*</sup> , NAL <sup>*</sup> , CHL <sup>*</sup> , ERY <sup>*</sup>	This study
AB766	Lung	Susceptible clinical isolates from HIA-Laveran, Marseille	
AB74	Lung	Clinical isolates from HIA-Laveran, Marseille: ZDM <sup>r</sup> , DOX <sup>r</sup> , NOR <sup>*</sup> , NAL <sup>*</sup> , ERY <sup>*</sup>	
AB66	Lung	Clinical isolates from HIA-Laveran, Marseille: CIP <sup>r</sup> , TET <sup>r</sup> , TOB <sup>r</sup> , CTX <sup>r</sup> , ZDM <sup>r</sup> , AMK <sup>r</sup> , MERO <sup>r</sup> , NOR <sup>*</sup> , NAL <sup>*</sup> , CHL <sup>*</sup> , ERY <sup>*</sup>	
AB775	Blood	Clinical isolates from HIA-Laveran, Marseille: CIP <sup>r</sup> , TET <sup>r</sup> , CTX <sup>r</sup> , ZDM <sup>r</sup> , NOR <sup>*</sup> , NAL <sup>*</sup> , CHL <sup>*</sup> , ERY <sup>*</sup>	
AB878	Lung	Clinical isolates from HIA-Laveran, Marseille: CIP <sup>r</sup> , TET <sup>r</sup> , TOB <sup>r</sup> , CTX <sup>r</sup> , ZDM <sup>r</sup> , DOX <sup>r</sup> , AMK <sup>r</sup> , MERO <sup>r</sup> , NOR <sup>*</sup> , NAL <sup>*</sup> , CHL <sup>*</sup>	

Note: According to the European Committee on Antimicrobial Susceptibility Testing (EUCAST) and the Clinical and Laboratory Standards Institute (CLSI), strains that were classified as resistant are indicated by superscripted 'r'. The superscripted '\*' were assigned to antibiotics whose minimal inhibitory concentration (MIC) values were >32 µg/mL and not defined by EUCAST or CLSI. The antibiograms of mentioned clinical strains are given in the supplementary section in Supporting Information: Tables S1–S5.

Abbreviations: AMK, amikacin; AMP, ampicillin; CFX, cefoxitin; CHL, chloramphenicol; CIP, ciprofloxacin; CLN, clindamycin; COL, colistin; CTX, cefotaxime; DOX, doxycycline; ERY, erythromycin; GEN, gentamicin; IMI, imipenem; LNZ, linezolid; MERO, meropenem; MDR, multidrug-resistant; NAL, nalidixic acid; NEO, neomycin; NOR, norfloxacin; OFL, ofloxacin; PIP, piperacillin; TET, tetracycline; TOB, tobramycin.

**TABLE 2** MIC values for 5-FU and its derivatives against reference ESKAPE group bacteria.

Compounds tested	MIC values expressed in (µg/mL)						
	<i>Klebsiella pneumoniae</i> (ATCC 13883)	<i>Pseudomonas aeruginosa</i> (ATCC 10145)	<i>Enterobacter aerogenes</i> (ATCC 13048)	<i>Escherichia coli</i> (ATCC 11775)	<i>Acinetobacter baumannii</i> (ATCC 19606)	<i>Staphylococcus aureus</i> (ATCC 25923)	<i>Enterococcus faecium</i> (ATCC 19434)
5-FU	4	256	64	16	128	2	4
<b>3a</b>	>256	>256	>256	>256	>256	>256	>256
<b>3b</b>	128	128	128	128	128	>256	>256
<b>4a</b>	128	128	>256	64	128	4	16
<b>5a</b>	>256	>256	>256	>256	>256	64	64
<b>4b</b>	>256	>256	>256	128	16	2	2
<b>6a</b>	16	8	32	8	16	1	2
<b>5b</b>	>256	>256	>256	>256	>256	256	256
<b>6b</b>	16	64	64–128	16	16	4–8	8
<b>6c</b>	4	8	16	4	4	2	2–4
<b>6d</b>	>256	>256	>256	>256	>256	64	64
<b>6e</b>	>256	>256	>256	>256	>256	64	64
Control <sup>a</sup>	0.125	0.06	0.06	≤0.06	0.5	0.5–0.25	2

Abbreviations: 5-FU, 5-fluorouracil; MIC, minimal inhibitory concentration.

<sup>a</sup>Ciprofloxacin is used as the control drug.

Phe-Arg β-naphthylamide (PAβN; potency, 98%), a well-known efflux inhibitor (Supporting Information: Table S6). Interestingly, it was observed that when combined with 20 µg/mL PAβN (Sigma-Aldrich), none of the said compounds showed an increase in their susceptibility. Thereby, suggesting that these compounds might have a binding site different from that of PAβN.<sup>[36]</sup> Similar to the results of *S. aureus* and *E. aerogenes* efflux mutants, none of the 5-FU derivatives exhibited a visible difference in MIC among *P. aeruginosa mexAB-oprM* deleted mutants.

## 2.3 | Electron microscopy

### 2.3.1 | Morphology of self-assembly formed by active 5-FU derivatives

As observed from Figure 2, **6a**, **6b** and **6c** were capable of forming self-assemblies. The average size of the self-assemblies formed by **6a** (Figure 2a) was found to be 114.66 ± 36.17 nm, whereas that of **6b** (Figure 2b) was found to be 194.16 ± 25.56 nm. In both cases, uniformity in size could not be observed. This increase in size could be correlated to the presence of a differential alkyl side chain present in the spacer group of each compound. As the alkyl chain length increased, the size of the self-assemblies increased linearly. These findings were consistent with research by Oliver et al., who examined the impact of surfactant head group and alkyl chain length on the size and shape of self-assemblies. They claimed that for surfactants, an increase in alkyl chain length led linearly to an increase in the size of

its self-assemblies and the number of aggregations, which in turn contributed to an increase in the hydrophobic interactions between adjacent monomers.<sup>[37]</sup> Interestingly, the asymmetry of the spacer group in **6c** (Figure 2c) was found to reduce the average size of the self-assemblies (104.69 ± 8.25 nm). Furthermore, the globules generated by **6c** were considerably more uniform than those obtained with **6a** and **6b**. This study highlights the ability of these compounds to form self-assemblies, which could prove useful from the perspective of drug delivery in the future.

### 2.3.2 | Morphology of cells treated with active 5-FU derivatives

The ultrastructure of *S. aureus* and *E. coli* with and without active 5-FU derivatives are depicted micrographically in Figures 3 and 4, respectively. The ultrastructure of normal (untreated) *S. aureus* cells (Figure 3a) revealed spherical cells with a well-defined regular smooth membrane. As observed, the electron-dense outer edge of the cell wall was distinctively stained due to the general presence of teichoic acid, which has a higher affinity for the contrast agents used (yellow arrow).<sup>[38]</sup> Furthermore, cells that were just beginning to divide had regular septal fold formation, whereas dividing cells had complete septa formation (white arrows). These cells did not differ significantly from previously published data<sup>[39–42]</sup> confirming their suitability for use as a control for this experiment. It was observed that *S. aureus* cells were significantly affected when treated with **6a** (Figure 3b), **6b** (Figure 3c) and **6c** (Figure 3d). *S. aureus* cells treated with **6a** at MIC

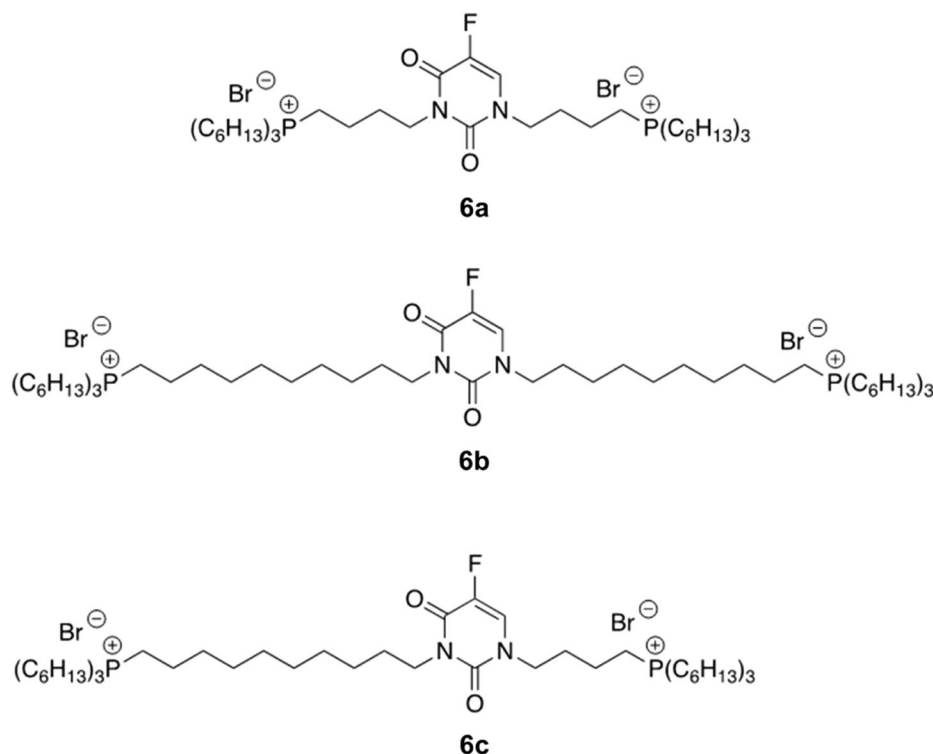


**FIGURE 1** Structure of active derivatives of 5-fluorouracil (**6a**, **6b** and **6c**).

concentration (Figure 3b) showed complete lysis of cells, most of the cells were found to be empty with their intracellular content completely leaked/dissolved (white asterisk). A few cells lost their spherical shape and became irregular. Some cells were also found to be abnormally enlarged with irregular bulging (blue asterisk) at the edges. At a lower concentration ( $\text{MIC} \times 0.5$ ), some cells showed space widening between two layers of the cell membrane. The widened gap (yellow arrow) seems to be filled with a homogeneous and electron-transparent substance which could be related to the violation of the molecular bonds between lipid layers, which could be induced by the increasing frequency of flip-flop events in the cells.<sup>[43]</sup> Some of the cells showed nonstraight septum (white arrow) along with the presence of electron-light regions in the cytosol. These regions had a fibre-like appearance (yellow triangle). Jensen et al.<sup>[44]</sup> reported a similar observation when *S. aureus* was treated with nisin. They inferred that it was most likely due to DNA condensation. At the lowest concentration tested ( $\text{MIC} \times 0.25$ ), **6a** did not induce profound septal or any membrane damage but showed the presence of concentric multimembrane structures (red dotted circle) varying in form and size. These concentric membranes were either electron dense or had an average electron density, and the space between them was filled with a homogeneous substance of average electron density that resembled the surrounding cytoplasm. As per studies conducted by Santhana Raj et al.<sup>[45]</sup> such formations could be the result of bacteria producing 'mesosomes' that were a defensive response to protect themselves from any antibiotic/toxin assault. Similarly, few researchers also observed such concentric multimembrane structures when *S. aureus* is treated with Gramicidin

*S.*<sup>[46]</sup> Riccardin C,<sup>[47]</sup> and defensin.<sup>[48]</sup> Interestingly, no visible damage to the membrane could be seen in cells treated with  $\text{MIC} \times 0.25$ . At the same time, these cells showed the presence of 'entangled fibres' (yellow triangle). Such fibre structures were observed in *S. aureus* cells after treatment with cationic peptides<sup>[40]</sup> and silver nanoparticles.<sup>[49]</sup> A similar effect was more evidently observed in cells treated with compound **6b** at MIC (Figure 3c). Although cells retain their spherical shape, cell wall and cell membrane, the presence of 'entangled fibres' were observed in almost all cells accompanied by the presence of vesicles. These vesicles were either filled with electron-dense grains or were 'empty' (red dotted circles). Unlike those observed in cells treated with **6a** cells treated with **6b** showed more hollow spaces, suggesting disruption/dissolution of in cytosolic matrix. The most striking feature was the presence of distinguishable 'serpentine' septum (white arrow). All these observations were found to be consistent irrespective of the concentration of **6b** used. Grigor'eva et al.,<sup>[40]</sup> reported that destroyed/serpentine septum were commonly observed with *S. aureus* cells treated with chlorhexidine; a cationic biguanide antimicrobial agent. Micrographs of *S. aureus* treated with compound **6c** at MIC (Figure 3d) revealed a few irregular and enlarged cells similar to those treated with **6a**. The septal division in these cells was found to crooked (white arrow) with few cells showing space widening between two layers of cell membrane (yellow arrow). Both concentric multimembrane structures and empty vesicles were seen (red dotted circle). In addition, many cells showed nonuniform distribution of charge in cytosols which appeared 'white spots' (white triangle). According to some reports, this is due to a change in the chemical properties of the



**TABLE 3** MIC ( $\mu\text{g/mL}$ ) values for 5-FU and its derivatives (without PA $\beta$ N).

Test compounds	MIC values expressed in ( $\mu\text{g/mL}$ )																	
	<i>Staphylococcus aureus</i>					<i>Enterobacter aerogenes</i>					<i>Pseudomonas aeruginosa</i>							
	<i>Escherichia coli</i>																	
SA-1199	SA-1199 B (Wild)	SAK-17589 ( $\Delta$ norA)	AG100 (Wild)	AG100A ( $\Delta$ acrAB)	AG102 (acrAB++)	AG100A <sub>TET</sub> (acrF+++)	EA27 (Wild)	EA289 (acrA++)	EA294 ( $\Delta$ acrA)	PAO1 (Wild)	PA402 ( $\Delta$ mexAB)	PW8749 ( $\Delta$ mexD)	PW5181 ( $\Delta$ mexF)	PT629 (mexAB+++)	ERY <sup>R</sup> (mexCD+++)	PAO-7H (mexEF+++)	CMZ091 (mexXY++)	PA403 ( $\Delta$ mexAB, CD, EF, XY, JK)
5-FU	0.25	0.5	1	16	8	8	256	128	64	512	512	512	>512	128	256	512	512	
<b>3a</b>	>512	>512	>512	>512	>512	>512	>512	>512	>256	>512	>512	>512	>512	>512	>512	>512	>512	
<b>3b</b>	Not evaluated as it precipitates in media over 128 $\mu\text{g/mL}$																	
<b>4a</b>	4	4	2	64	8	64	128	256	128	128	128	128	128	64	128	128	128	
<b>5a</b>	256	256	256	>512	512	>512	>512	>512	>512	>512	>512	>512	>512	>512	>512	>512	>512	
<b>4b</b>	2	4	2	16	2	32	32	>512	>512	512	512	512	512	256	512	512	512	
<b>6a</b>	2	2	2	8	8	8	64	64	32	32	32	32	32	16	16	32	32	
<b>5b</b>	>512	>512	>512	>512	>512	>512	>512	>512	>512	>512	>512	>512	>512	>512	>512	>512	>512	
<b>6b</b>	1	1	1	32	16	32	32	32-16	16	64	64	8	64	64	64	64	64	
<b>6c</b>	0.5	1	0.5	4	2	2	2	8	8	8	8	8	16	16	16	8	16	
<b>6d</b>	64	64	32	>512	64	>512	64	>512	>512	512	512	512	512	512	512	512	512	
<b>6e</b>	4	4	4	>512	512	>512	512	>512	>512	512	512	512	512	512	512	512	512	
Control <sup>a</sup>	1	64	0.5	8	2	32	64	256	1024	32	32-64	16	16	64-128	16	64	32	

Abbreviations: 5-FU, 5-fluorouracil; MIC, minimal inhibitory concentration; TET, tetracycline.

<sup>a</sup>Control drug used for *S. aureus*: norfloxacin, *E. coli*: nalidixic acid, *E. aerogenes*: chloramphenicol, *P. aeruginosa*: doxycycline.

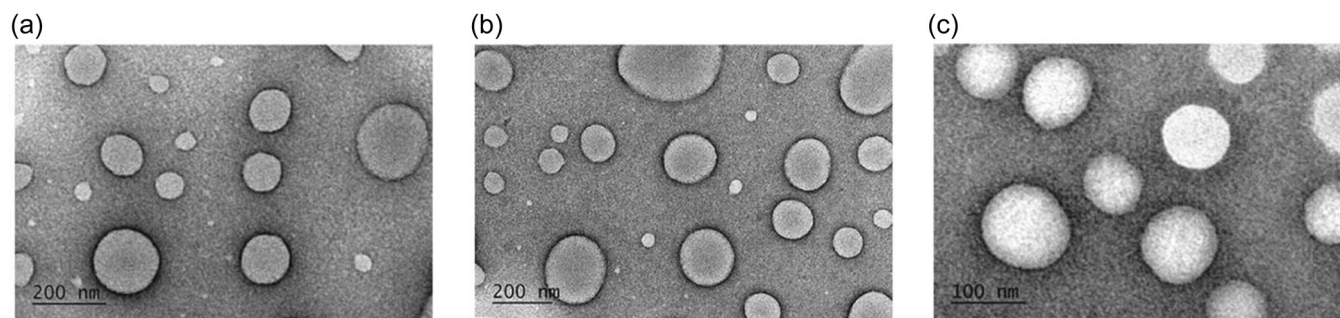


**FIGURE 2** Self-assembly formed by (a) **6a**, (b) **6b** and (c) **6c**.

cytoplasmic composition. However, unlike in our case, reports have found the spots to be darker. There have currently been no reports or observations of white spots. Thus, this observation can be loosely based on the idea that there might be some change in chemical properties of cytoplasm. Cells treated with **6c** at MIC  $\times 0.5$  concentration showed intact cell membranes with a more prominent fibre-like structure (yellow triangle), implying DNA condensation. Although no empty vesicles were seen, the septum was found to be abnormally wide and blurry (white arrow), with no discernible mid-line. White spots (white triangle) were seen in a few cells. Cells with the lowest concentration of **6c** tested had smooth regular cell membranes, with only a few cells having a disrupted septum. However, white spots (white triangles) indicating cytoplasmic alteration were still evident.

These active compounds were also tested against Gram-negative *E. coli* bacteria. The ultrastructure of *E. coli* is depicted in Figure 4a. Control cells (untreated) were found to be rod or ellipsoidal with a distinct cell wall. The cell membrane (white arrow) connected to the cytoplasm and the cell wall (yellow arrow) seemed to be separated by an electro-translucent layer. The lighter electron density in the cell indicated the presence of a nucleoid region consisting of naked DNA (yellow asterisk). The granular electron-dense region marked the presence of ribosomes (yellow asterisk). This structure corresponded to control images observed in several pieces of the reported literature.<sup>[50–53]</sup> However, the morphology of cells changed when treated with **6a** at MIC (Figure 4b). Although cells showed smooth and continuous cell walls, one can notice the presence of ‘plasmolysis space’ (yellow triangle) within the cell. These plasmolytic spaces were more likely generated on the apical region. It has been observed that treatment of cationic peptides,<sup>[54]</sup> plant extracts,<sup>[52,55]</sup> silver ions,<sup>[56]</sup> and honey<sup>[51]</sup> has been shown to induce the formation of such plasmolytic regions in *E. coli*. A few membrane-bound white vesicles (dotted yellow circle) were also seen. Furthermore, the darker patch within the plasmolysis space may be an exocytotic vesicle or the result of the outpouching of the cell membrane (dotted red circle). Schwarz and Koch<sup>[53]</sup> made a similar finding while studying osmotically stressed *E. coli* cells in their research. They concluded that the formation of endocytic vesicles develops because phospholipid membranes have a limited capacity

to contract, necessitating the removal of extra membranes to create plasmolysis gaps. Cells treated with **6a** at MIC  $\times 0.5$  showed some presence of laminar plasmolysis space (white triangle) along with previously observed defects. At MIC  $\times 0.25$ , cells showed the presence of endocytic vesicles but outpouching was rarely seen. Cells treated with **6b** at MIC, MIC  $\times 0.5$  and MIC  $\times 0.25$  (Figure 4c) exhibited similar results. Interestingly, cells treated with **6c** at MIC showed the presence of extracellular matter (Figure 4d). Despite the fact that none of the cells were empty or lysed, their cytosol was abnormally electron dense. At all tested concentrations of **6c**, cells showed the presence of plasmolytic regions and irregular entangled fibre-like structures (red arrow). At MIC  $\times 0.25$ , concentric multilayered vesicles similar to those found in *S. aureus* were observed. Weigand et al.<sup>[50]</sup> observed a similar effect in cells exposed to high temperature and alluded to them as ‘whorls’. They concluded that these whorls are extra membrane production and are linked to disruptions in membrane production during the growth phase. Vetterli et al.<sup>[57]</sup> observed similar whorls after treating cells with thanatin. They demonstrated that these formations occur as a result of lipopolysaccharide transport and outer membrane biogenesis inhibition in *E. coli*. However, unlike cells treated with **6c** at MIC or MIC  $\times 0.5$ , laminar and apical plasmolysis was uncommon. Furthermore, a few cells showed dark spots (red asterisk), which may indicate the presence of phosphate bodies.

## 2.4 | Effect of active 5-FU derivatives on clinical strains

Clinical strains used in this experiment are enlisted in Table 1. The MIC values of **6a**, **6b** and **6c** on the clinical isolates of Gram-positive bacteria (*S. aureus*) and Gram-negative bacteria (*E. coli*, *A. baumannii*, *P. aeruginosa* and *K. pneumoniae*) are depicted in Figure 5a–e. For *S. aureus*, compound **6a** exhibited the lowest MIC (0.5–1  $\mu\text{g}/\text{mL}$ ) followed by **6c**, which exhibited an MIC of 1  $\mu\text{g}/\text{mL}$  in all the tested clinical strains of *S. aureus* irrespective of its resistance. **6b** demonstrated a higher MIC (1–4  $\text{g}/\text{mL}$ ). In Gram-negative isolates, when compared to **6a** and **6c**, the MIC values of compound **6b** were found to be higher against the clinical strains of *E. coli* (16–32  $\mu\text{g}/\text{mL}$ )

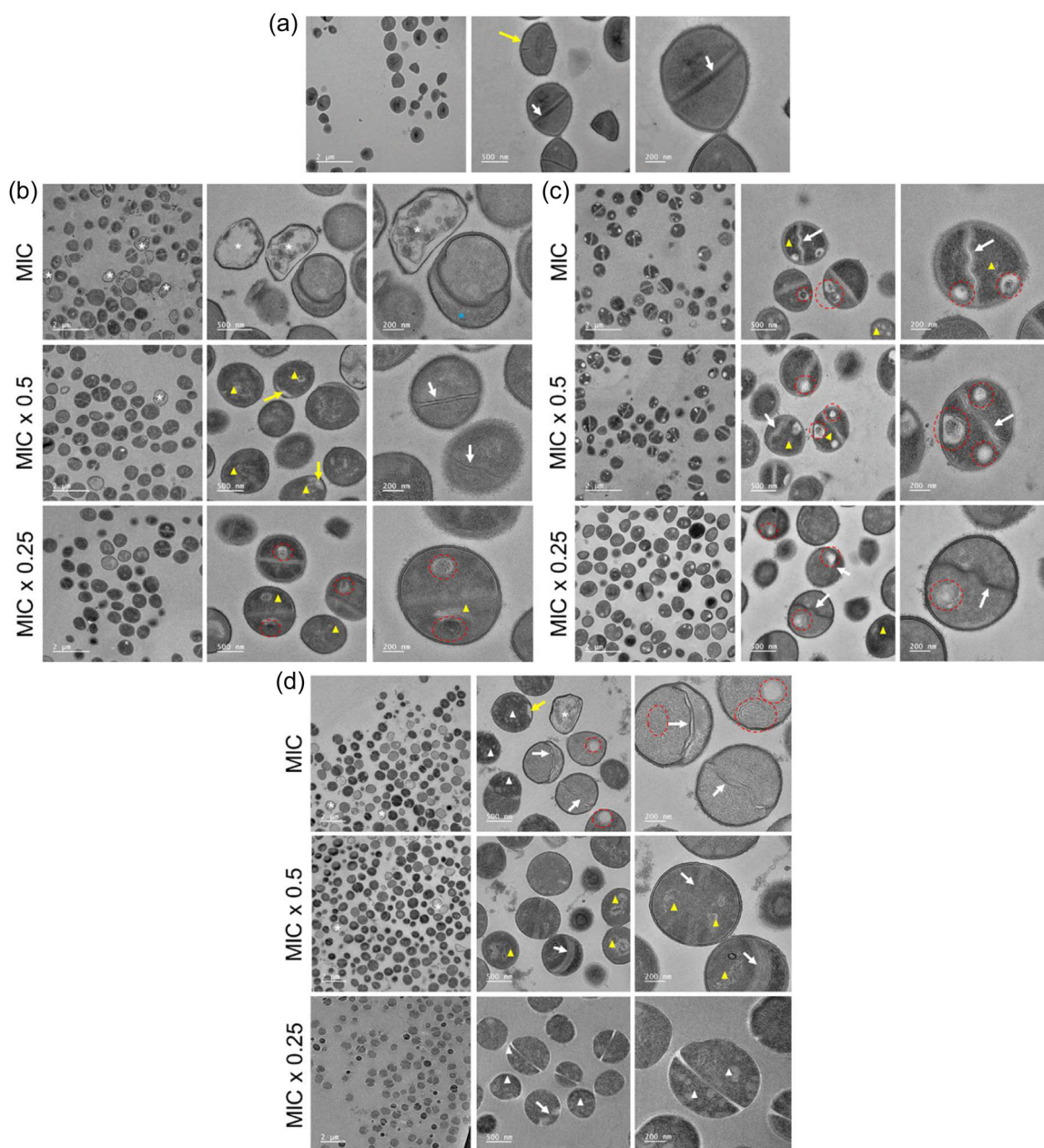


**FIGURE 3** Transmission electron microscopy (TEM) micrographs of (a) untreated *Staphylococcus aureus* cells; (b) cells treated with different concentrations of **6a** (MIC, MIC  $\times$  0.5 and MIC  $\times$  0.25); (c) cells treated with different concentrations of **6b** (MIC, MIC  $\times$  0.5 and MIC  $\times$  0.25); and (d) cells treated with different concentrations of **6c** (MIC, MIC  $\times$  0.5 and MIC  $\times$  0.25). The white arrows in the images indicate the cell septum, while the yellow arrows indicate the cell membrane. The white asterisk (\*) signifies cell lysis/empty cells, while the blue asterisk (\*) denotes a bulging area. The yellow triangles represent entangled fibre-like structures, whereas the white triangle depicts the probable change in cytoplasmic composition. Dotted red circles represent concentrated multimembrane structures or empty vesicles.

and *P. aeruginosa* (32–64  $\mu\text{g}/\text{mL}$ ). Similar to that of *S. aureus*, the MIC values of **6c** were found to be the same for all tested *E. coli* (4  $\mu\text{g}/\text{mL}$ ). **6a** exhibited MIC ranging from 8 to 16  $\mu\text{g}/\text{mL}$  against *E. coli*. MIC values of **6a** and **6c** were fairly similar against clinical isolates of *P. aeruginosa* (8–16  $\mu\text{g}/\text{mL}$ ). Interestingly, MIC values of **6a** (4–32  $\mu\text{g}/\text{mL}$ ) were found to be higher for *A. baumannii* followed by **6b** (8–16  $\mu\text{g}/\text{mL}$ ) and **6c** (4–8  $\mu\text{g}/\text{mL}$ ). Also, in the case of *K. pneumoniae*, **6a** and **6b** exhibit more or less similar activity. Overall, **6c** had lower MIC values in both Gram-positive ( $\leq 1$  g/mL) and Gram-negative

( $\leq 16$  g/mL) bacteria. Our findings were encouraging given that Gieringer et al.<sup>[58]</sup> observed that the MIC values of 5-FU against clinical Gram-negative isolates (*K. pneumoniae* and *P. aeruginosa*) were  $>100$   $\mu\text{g}/\text{mL}$  and that the observed MIC could only be decreased after 5-FU was combined with  $\beta$ -lactam antibiotics. Furthermore, the MIC values for **6c** did not differ from those obtained with reference strains. This suggests that **6c** may have possibly overcome the resistance mechanism that exists within tested clinical strains. Therefore, **6c** was selected for further testing.

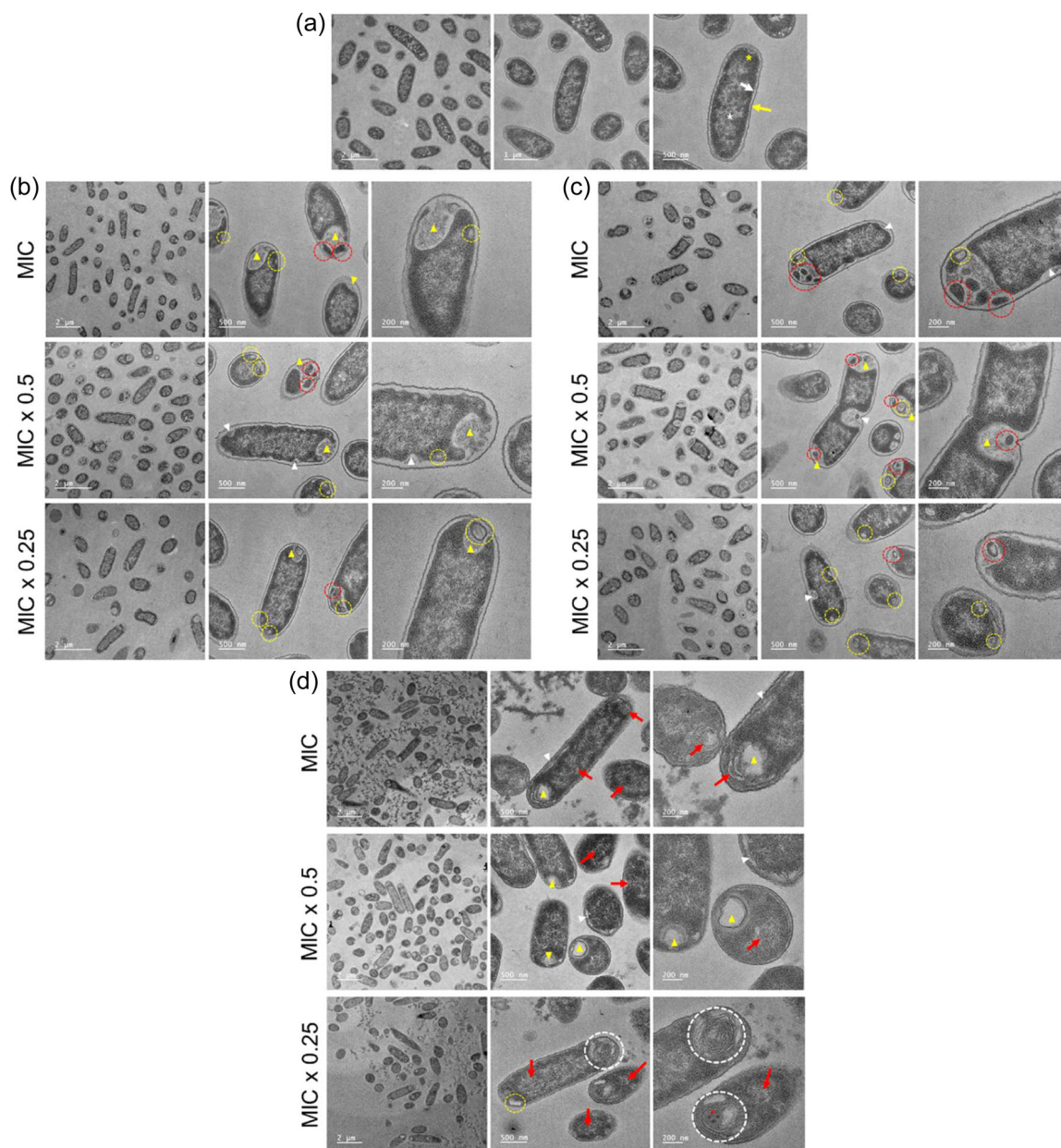


**FIGURE 4** Transmission electron microscopy (TEM) micrographs depicting (a) control *Escherichia coli* cells (untreated), (b) *E. coli* cells treated with different concentrations (MIC, MIC  $\times$  0.5 and MIC  $\times$  0.25) of **6a**, (c) *E. coli* cells treated with different concentrations (MIC, MIC  $\times$  0.5 and MIC  $\times$  0.25) of **6b**, (d) *E. coli* cells treated with different concentration (MIC, MIC  $\times$  0.5 and MIC  $\times$  0.25) of **6c**. In control images, the white arrow and yellow arrow signify the cell's inner and outer membrane, respectively. The white and yellow asterisk (\*) show cytosolic region and ribosomes, respectively. In the treated cells, apical and laminar plasmolytic areas are marked by yellow and white triangles, respectively. The membrane-bound endocytic vesicles and outpouching of the cell membrane are highlighted by a yellow and red dotted circle, respectively. The red arrow shows irregular entangled fibre-like structure 'whorls', and the red asterisk shows the presence of phosphate bodies.

## 2.5 | Membrane permeabilization assays

The transmission electron microscopy (TEM) micrographs revealed that the treated cells had cytoplasmic and septal anomalies, indicating DNA condensation and cell division defects, respectively. Furthermore, cells treated with **6c** formed whorls or multilayered vesicles, indicating possible membrane formation issues. As a result, the authors decided to investigate the effect of **6c** on the membrane

permeability of Gram-positive and Gram-negative bacteria. Permeability of Gram-positive bacteria (*S. aureus* SA1199) was carried out by using propidium iodide (PI) (Sigma-Aldrich). PI is a membrane-impermeable stain that only produces fluorescence after binding to double-stranded DNA. Hence, it serves as a marker for membrane disruption or permeation. As observed from Figure 6a, MIC  $\times$  2 ( $p < 0.001$ ) and MIC ( $p < 0.05$ ) concentrations caused a significant membrane perturbation in *S. aureus* bacteria as compared to

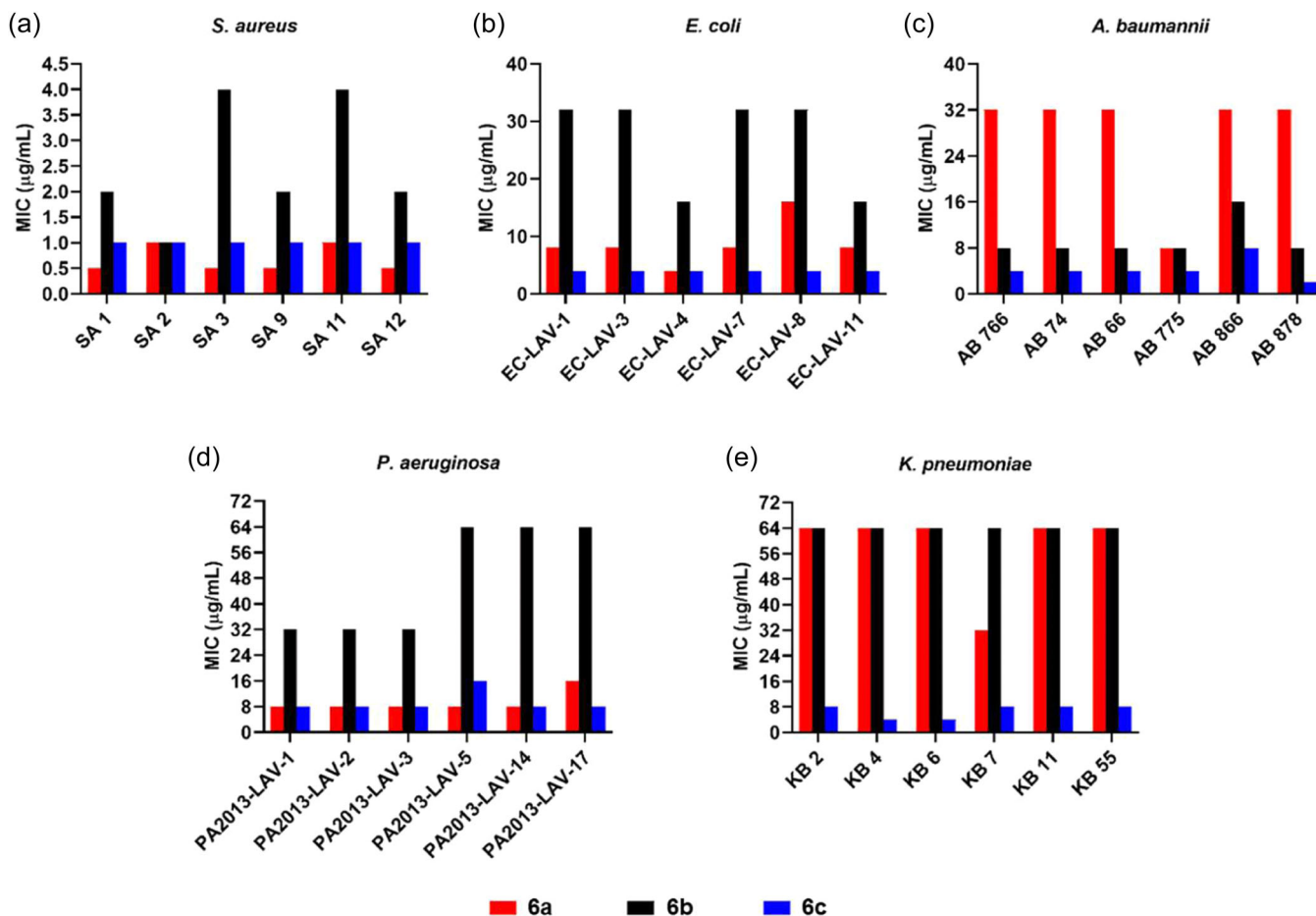


**FIGURE 5** Bar graph representing the effect of **6a** (red bar), **6b** (black bar) and **6c** (blue bar) on clinical strains of (a) *Staphylococcus aureus*, (b) *Escherichia coli*, (c) *Acinetobacter baumannii*, (d) *Pseudomonas aeruginosa*, (e) *Klebsiella pneumoniae*. Details of clinical strains used in this experiment are listed in Table 1.

phosphate-buffered saline (PBS). However, thereafter decreasing **6c** concentration resulted in nonsignificant permeabilization in *S. aureus*.

The effect of compound **6c** on outer membrane permeabilization (OMP) of a Gram-negative bacteria was evaluated in *E. coli* (T-AG 100, AG100 cells transformed with pACYC184-amp<sup>R</sup>C) and *E. aerogenes* EA289. Nitrocefin, a  $\beta$ -lactamase hydrolysable molecule (Oxoid™; Thermo Fisher Scientific Inc.™) was used to determine OMP. In this experiment, polymyxin B (PMB) was employed as a positive control. The permeabilization of the outer membranes by PMB was shown to be relatively stable after 16  $\mu$ g/mL for both *E. coli* and *E. aerogenes*, hence a concentration of 16  $\mu$ g/mL of PMB was regarded to yield 100% OMP (data not shown). The %OMP induced by PMB in *E. coli* (Figure 6b) bacteria reduced abruptly after 1  $\mu$ g/mL, in contrast to the response observed in *E. aerogenes* bacteria wherein a steady decrease in %OMP was observed (Figure 6c). The %OMP induced by **6c** in *E. coli* bacteria (Figure 5b) decreased when **6c** concentrations were decreased. At twice the MIC concentration, %OMP induced by **6c** ( $82.993 \pm 2.14$ ) was found to be comparable to PMB (1  $\mu$ g/mL) ( $82.600 \pm 6.86$ ), which then decreased ( $56.424 \pm 4.56$ ) at the MIC concentration. Similarly, to the response seen with PMB, a decrease in **6c** concentrations caused an abrupt drop in %OMP at MIC  $\times 0.5$  and

lower concentrations ( $\leq 10\%$ ). In *E. aerogenes*, **6c** produced a dose-dependent decrease in %OMP (Figure 5c). The permeabilization of the outer membrane caused by **6c** (MIC  $\times 2$ ) ( $41.418 \pm 4.56$ ) was comparable to that caused by PMB (2  $\mu$ g/mL) ( $43.539 \pm 6.73$ ), while the permeabilization caused by MIC was found to be  $30.358 \pm 3.04\%$ . At MIC  $\times 0.5$ , %OMP was found to be  $16.615 \pm 3.706$ , which was comparable to PMB (1  $\mu$ g/mL,  $17.698 \pm 0.54$ ). Furthermore, a reduction in **6c** resulted in  $<15\%$  OMP. Considering the results obtained in both the test bacteria, **6c** produced a pronounced effect on the outer membrane of bacteria at MIC or higher concentration. Borselli et al.<sup>[59]</sup> summarized that compounds that cause even a small breach in the membrane may permit the passage of an electric current that depolarizes the inner membrane of Gram-negative bacteria without permitting the passage of larger molecules. Membrane potential shifts may interfere with free energy, which enables cells to do chemical and mechanical work such as ATP synthesis.<sup>[60]</sup> However, it was revealed that compound **6c**, at MIC  $\times 2$  and MIC concentrations, induced less than 15% of inner membrane depolarization in both *E. coli* (Supporting Information: Figure S16a) and *E. aerogenes* (Supporting Information: Figure S16b). Since then, a further drop in MIC has had no discernible impact on membrane depolarization. This concludes that depolarization

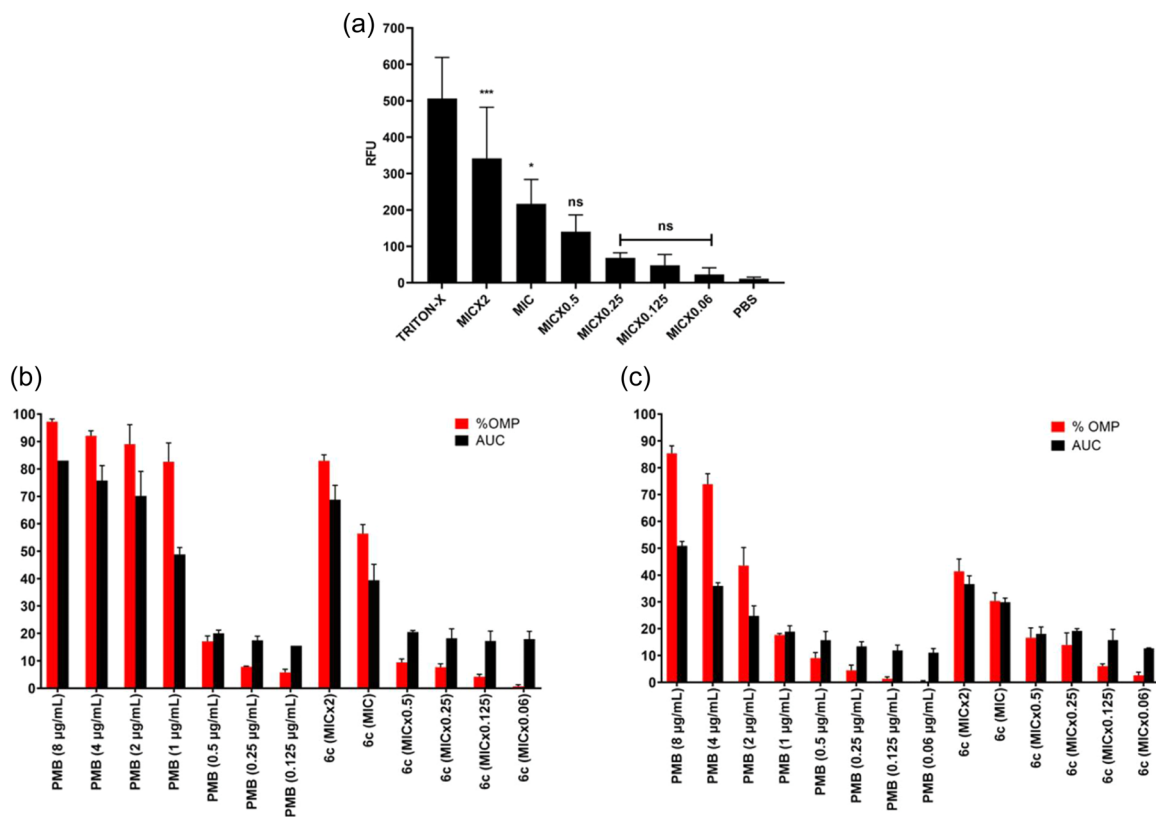


**FIGURE 6** (a) The membrane permeability of *Staphylococcus aureus* caused by different concentrations of 6c in (SA-1199) using the propidium iodide (PI) assay. Statistical significance (\* $p < 0.05$ ; \*\*\* $p < 0.001$ ) was determined using one-way analysis of variance (ANOVA) in multiple comparisons with reference phosphate-buffered saline, pH 7.4 (PBS). (b) Results of nitrocefin hydrolysis assay in *Escherichia coli* (T-AG 100) and (c) *Enterobacter aerogenes* (EA289) are represented by a bar graph. In this figure, the red bar represents the percent outer membrane permeability (% OMP) at the time interval of 60 min, and the black bar represents the area under the curve (AUC) obtained from the kinetic experiment conducted for 60 min.

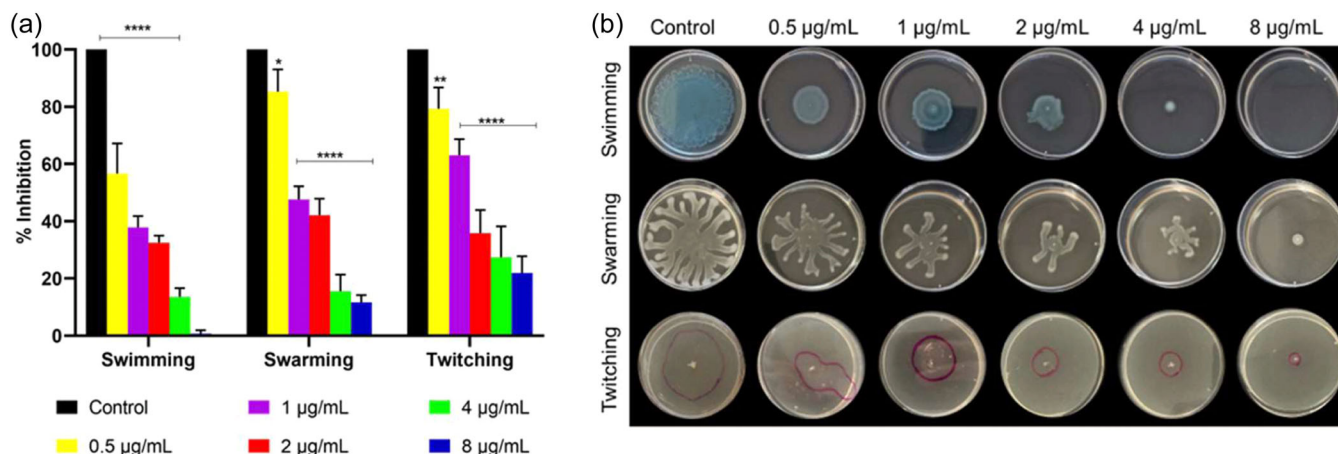


**FIGURE 7** (a) Bar graph showing a statistical comparison of different concentrations of 6c on the motility of the *Pseudomonas aeruginosa* (PAO1) strain. (b) Image of results of swimming, swarming and twitching. The minimal inhibitory concentration (MIC) value of 6c (8 µg/mL) on PAO1 was deduced by the microbroth dilution method in MH-II broth. All experiments were done at least three times, and statistical significance was determined using one-way analysis of variance (ANOVA) (\* $p < 0.05$ ; \*\* $p < 0.01$ ; \*\*\* $p < 0.001$ ; \*\*\*\* $p < 0.0001$ ). Twitching results being very faded is outlined by a marker.

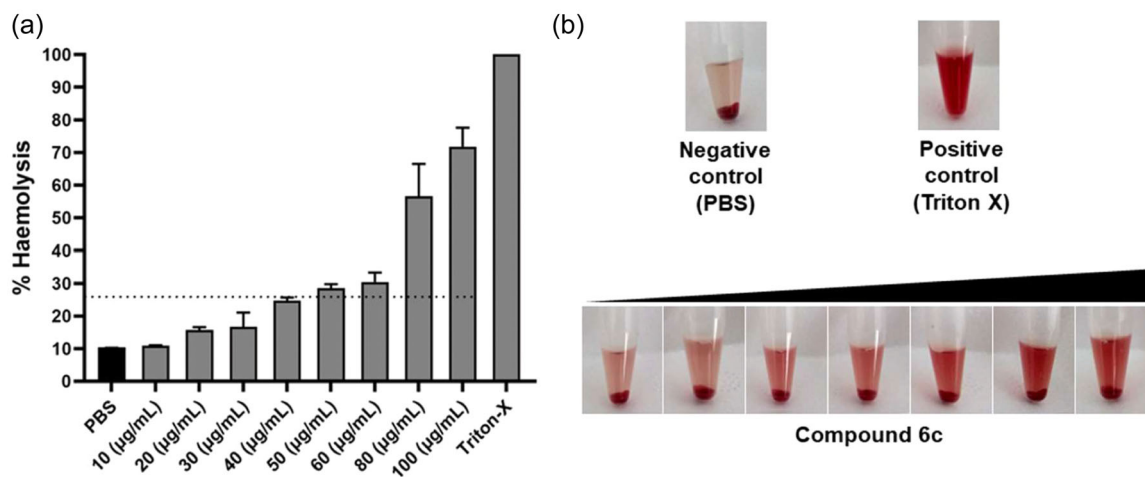


**FIGURE 8** (a) Bar graph and (b) image depicting % haemolysis caused by different concentrations of **6c** (10–100 µg/mL) in comparison to the positive control (1% w/v Triton-X) and negative control (phosphate-buffered saline [PBS], pH = 7.4).

is not a clear mechanism of action for **6c**. Based on the observed results, one can speculate on the reason for **6c**'s failure to inhibit the efflux mechanism in bacteria. Depolarization would have de-energized the efflux pump since it is powered by a proton gradient across the inner membrane, which would have increased the efficiency of **6c** in test efflux mutants, which was not observed.

## 2.6 | Motility assays

Bacteria have evolved a diverse set of motility mechanisms to take advantage of available nutrients and their surroundings. Bacterial motility plays a key role in its virulence and antibiotic resistance. *P. aeruginosa* bacteria approach a surface using swimming motility mediated by flagella, adhere and then spread further via surface-associated motilities known as swarming and twitching, mediated by numerous flagella and type IV pili, respectively.<sup>[61]</sup> Figure 7a,b demonstrates the effect of inhibitory and subinhibitory concentrations of **6c** on the motility of *P. aeruginosa* (PAO1). As observed, the rotating flagellar movements of individual bacteria, known as swimming motility, were significantly ( $p < 0.0001$ ) inhibited even in the presence of the lowest concentration of **6c** tested (0.5 µg/mL). Similarly, swarming motility, characterized by the formation of complex dendritic, fractal-like patterns, could be seen to be significantly ( $p < 0.05$ ) inhibited by **6c** at 0.5 µg/mL and more profoundly ( $p < 0.0001$ ) at concentrations higher than 1 µg/mL. These findings imply that **6c**, at MIC (8 µg/mL) and subinhibitory concentrations, inhibits both *P. aeruginosa*'s rotatory and oscillatory flagellar motility, making bacterial migration difficult. In 2009, Ueda et al.<sup>[16]</sup> concluded that uracil biosynthesis was important for swarming regulons and some quorum sensors. They observed that 5-FU effectively suppressed these quorum sensors, inhibiting swarming-related motility in *P. aeruginosa*. Additionally, Dimmit et al.<sup>[62]</sup> found that adding 5-FU to bacterial cultures resulted in the synthesis of aberrant flagellin protein, resulting in abnormal flagellar motility. Additionally, Kerr<sup>[63]</sup> found that 5-FU can effectively delay flagellum morphogenesis in *Didymium*

*nigripes*. In light of these findings, it is plausible that our compound, **6c**, may have exhibited similar effects due to the presence of a 5-FU ring in its structure. Interestingly, twitching motility is independent of the presence of a flagellum and solely depends on the presence of retractile type-IV pili. However, it was found that twitching motility was considerably inhibited ( $p < 0.01$ ) at the tested lowest **6c** concentration (0.5 µg/mL). In 2022, Niazy et al.<sup>[64]</sup> conducted experiments comparing the motility of reference *P. aeruginosa* and *pyrE* gene knockout mutants of *P. aeruginosa* ( $\Delta pyrE$ ). They observed that the deletion of the *pyrE* gene rendered *P. aeruginosa* uracil scavengers and arrested their twitching motility. They concluded that pyrimidine synthesis is crucial for *P. aeruginosa* motility. Furthermore, several studies revealed that 5-FU inhibited pyrimidine synthesis in *Pseudomonas* species and reduced quorum sensing and biofilm growth via uracil-related mutations in *carA*, *carB*, *pyrB*, *pyrC*, *pyrD*, *pyrE* and *pyrF*.<sup>[16,65,66]</sup> As a result, it is probable that **6c** altered pyrimidine synthesis, which in turn affected PAO1's twitching ability. These findings are intriguing since **6c** altered bacterial surface translocation, which may later establish the foundation for its potential to decrease biofilm formation.

## 2.7 | Haemolytic activity

Red blood cells (RBCs) are frequently used as a model for mammalian cell membranes and the inner and outer leaflet compositions. Given the ease of isolating erythrocytes, the haemolytic activity assay provides a useful technique for rapid initial toxicity assessment. Many compounds can solubilize RBC membranes, causing the oxygen-carrying pigment haemoglobin to be released into the surrounding media, which can be evaluated as a toxicity response. As seen from Figure 8b, there is no release of haemoglobin in the presence of PBS, pH 7.4, whereas in the presence of 1% w/v Triton-X, a known surface-active agent, RBCs completely burst open (*note*: no cell pellet observed after complete bursting of RBC). It was illustrated in Figure 8a that **6c** exhibited nonhaemolytic activity at 50 µg/mL (% haemolysis = 23.062 ± 0.01).

When compared to the MIC values of CA-27 (the highest MIC was found for *E. aerogenes* is 16 µg/mL), the haemolytic concentrations are >threefold higher, suggesting that the compound is safe and efficient.

### 3 | CONCLUSION

The effects of phosphonium-based 5-FU derivatives on Gram-positive and Gram-negative bacteria are highlighted in this investigation. The study shows that tri-hexylphosphonium substitution on both nitrogen of the 5-FU skeleton is required for antibacterial activity against both Gram-positive and Gram-negative bacteria. Furthermore, asymmetric spacer groups were found to improve the antibacterial properties of phosphonium-based 5-FU derivatives. Active 5-FU derivatives were found to have a considerable effect on cell division and cytoplasmic composition in *S. aureus*. In *E. coli*, these compounds triggered plasmolysis as well as the formation of vesicles within the cytoplasm, indicating cytoplasmic disintegration and phospholipid membrane contraction. Furthermore, both *S. aureus* and *E. coli* cells had fibre-like strands and concentric vesicles, which could indicate DNA condensation and stress responses, respectively. However, more research is needed to corroborate these findings. Interestingly, in accordance with the microscopy findings, **6c** generated considerable membrane disruption or depolarization only at MIC doses. Cell membranes appeared to be unaffected at lower doses than MIC. To conclude, the mechanism of action of phosphonium-based 5-FU derivatives on Gram-positive bacteria primarily involves disrupting cell division and triggering cytosolic matrix change. At MIC concentration, it induces membrane perturbation in *S. aureus* cells. In Gram-negative bacteria (*E. coli*), these compounds essentially cause plasmolysis, with only compound **6c** showing additional evidence of disruptions in membrane production. Regardless of the clinical strain resistance profile, the most active compound, **6c**, displayed consistent MIC values, suggesting its efficiency in treating drug-resistant bacteria. It was intriguing to find that **6c** had a considerable influence on bacterial motility, implying that it may be used as an antibiofilm agent. Although present research is focused on the antibacterial activity of phosphonium-based 5-FU derivatives, the possibility of 5-FU derivatives being combined with conventional antibiotics will be investigated in the future. Furthermore, the nonhaemolytic and self-assembling capabilities of **6c** may pave the way for the development of phosphonium-based 5-FU nanovesicles for AMR drug delivery.

## 4 | EXPERIMENTAL

### 4.1 | General procedure for the synthesis and characterization of 5-FU derivatives

#### 4.1.1 | Synthesis of mono-phosphonium salts

First, the N1-position of 5-FU was protected by the tBoc protective group using Boc<sub>2</sub>O in CH<sub>3</sub>CN to give **1** in 63% yield. Then, treatment of **1** with NaH in DMF followed by the addition of di-bromoalkanes allowed the alkylation N3-position giving the two intermediaries **2a** and **2b** in

moderate yields. Compound **2** underwent the usual deprotection of N-tBoc by K<sub>2</sub>CO<sub>3</sub> in MeOH and gave **3a** and **3b** in excellent yields. The last step was a microwave-assisted phosphorylation of **3** using tri-alkylphosphine in acetonitrile for 4 h at 85°C. According to this route, the two mono-phosphonium salts **4a** and **4b** were obtained in good yields.

#### 4.1.2 | Synthesis of di-phosphonium salts

This strategy could be extended to synthesise a first asymmetric di-phosphonium target **6c** bearing two alkyl chains of different lengths (C10 and C4). Thus, the free N1-position of **3b** was alkylated with 1,4-dibromobutane in a NaH suspension in DMF and afforded di-brominated compounds **5c** in 52% yield. Finally, **5c** was di-phosphorylated according to the aforementioned microwaves-assisted protocol and led to the target **6c** in good yield. Four other symmetrical di-phosphonium salts bearing identical alkyl chains (C4 or C10) could be synthesised directly from 5-FU. The commercial product underwent a double N-alkylation after treatment with NaH followed by the addition of 4 eq. of di-bromoalkanes (1,4- or 1,10-dibromoalkane). Finally, compounds **5** obtained in moderate yields were di-phosphorylated with 4 eq. of several tri-alkylphosphines (P(Hex)<sub>3</sub>, P(But)<sub>3</sub> and P(Oct)<sub>3</sub>) affording targets **6a**, **6b**, **6d** and **6e** only in a two-step sequence.

#### 4.1.3 | Characterization of the 5-FU derivatives

All compounds were characterized by <sup>1</sup>H NMR, <sup>13</sup>C NMR, <sup>31</sup>P NMR and mass spectroscopy. <sup>1</sup>H NMR and <sup>13</sup>C NMR spectra were recorded at 20°C on a Bruker spectrometer at 250 MHz (<sup>1</sup>H) and 62.5 MHz (<sup>13</sup>C). Chemical shifts are given in ppm referenced to the solvent residual peak (<sup>1</sup>H, CDCl<sub>3</sub>, 7.26 ppm; and <sup>13</sup>C, 77 ppm). <sup>1</sup>H NMR coupling constants (*J*) are reported in Hertz. Electrospray ionization mass spectra (ESI-MS) and elemental analyses were performed at the spectropole of the Faculté des Sciences et Techniques de Saint Jérôme, Marseille, France. ESI-MS was recorded with an API/Plus Sciex triple quadrupole spectrophotometer in the positive mode. Analytical thin layer chromatography (TLC) was performed on precoated glass plates with Kieselgel 60 F254 neutral with an aluminium support plate (0.25 mm), SDS. Compounds were revealed by UV light (254 nm) after spraying with 5% sulphuric acid ethanol solution and heating. Column chromatography was performed on Merck silica gel 60 (0.063–0.200 mm) or silica gel reverse phase C18.

The InChI codes of the investigated compounds, together with some biological activity data, are provided as Supporting Information.

### 4.2 | Susceptibility assays

#### 4.2.1 | Susceptibility testing on ESKAPE group bacteria

The MIC of 5-FU derivatives was performed according to the Clinical and Laboratory Standards Institute (CLSI) guidelines M07-A9<sup>[67]</sup> using the microbroth dilution methods. The broth microdilution tests were



performed in sterile, flat-bottomed, 96-well microplates (Corning™ CoStar™ Merck). The test was performed by the BAC-SCREEN platform in our lab. Briefly, 5-FU derivatives were solubilized in dimethyl sulphoxide (DMSO) and further diluted with sterile distilled water to obtain twofold serial dilutions ranging from 128 to 0.25 µg/mL. The final test concentration consisted of <1% w/v DMSO. An aliquot (100 µL) of the prepared concentrations was transferred to the well of the microplate. Optimally, within 15 min of preparation, the inoculum was adjusted in Muller Hinton (MH-I) cation-adjusted (MH-II) broth purchased from Merck Millipore to obtain approximately  $5 \times 10^5$  CFU/mL. *E. faecium* was adjusted in MH-I supplemented with 5% of defibrinated horse blood and 20 mg/L of β-nicotinamide adenine dinucleotide. The prepared inoculum (100 µL) was then transferred to each well of the microplate. The plates were incubated for 18 h at 37°C. To indicate bacterial growth, lodonitrotetrazolium chloride (INT) purchased from Tokyo Chemical Industry Co., Ltd. (TCI, Europe N.V.) was used. An aliquot of 40 µL of 0.2 mg/mL INT solution was added to each well. All MIC determinations were repeated at least three times in an independent experiment.

#### 4.2.2 | Susceptibility testing on efflux mutants

Similar to the susceptibility testing on ESKAPE group bacteria, MIC values were determined against efflux mutants enlisted in Table 1. The compounds that showed differential MIC values than their respective parent (wild) strains were then retested in the presence of 20 µg/mL of a well-known efflux pump inhibitor called PAβN.<sup>[27,68]</sup>

### 4.3 | Electron microscopy

#### 4.3.1 | Morphology of self-assembly formed by active 5-FU derivatives

The ability of 5-FU derivatives to self-assemble was examined using TEM. An aliquot (20 µL) of an aqueous suspension (100 µg/mL) of **6a**, **6b** and **6c** was placed on a 300-mesh copper grid covered by a thin amorphous carbon film for electron microscopy. Negative staining was achieved by adding 10 µL of 1% w/v aqueous ammonium molybdate solution. Measurements were carried out using a Philips CM10 TEM (FEI Company) operated at 80 kV and images were recorded by the 2k × 2k side 27-mounted Veleta CCD camera (Olympus).

#### 4.3.2 | Morphology of cells treated with active 5-FU derivatives

The ultrastructural changes within the bacterial cells before and after treatment with active 5-FU derivatives (**6a**, **6b** and **6c**) were observed using an FEI Tecnai G2-20 TWIN TEM with a 200 kV field emission and a Gatan Oneview camera (4 K × 4 K). Briefly, mid-log phased cell

suspensions of *S. aureus* (ATCC 25923) and *E. coli* (ATCC 11775) were incubated separately at 37°C for 4 h with test concentrations of 5-FU derivatives (MIC × 2, MIC and MIC × 0.5). Untreated cells serve as a control. Postincubation for 4 h, cells were harvested by centrifugation (4500 rpm, 10 min) and primed at 22°C by adding an equal volume of 2% glutaraldehyde prepared in PBS, pH = 7.4. After 20 min, the medium was replaced with 1% glutaraldehyde and incubated for another 1 h at 4°C. Cells were then washed with PBS and concentrated in 2% agarose (LMP Agarose; Sigma-Aldrich). To postfix the cells, 1% Osmium Tetroxide (EMS 19150) was added, and the samples were left at room temperature for 1 h. Samples were again washed in distilled water and treated with 1% uranyl acetate (EMS 22400) for 1 h at 4°C in the dark. The samples were then dehydrated with graded ethanol solutions, embedded in Epon (Polysciences 8792), and left to polymerize over the weekend. From each sample, ultrathin sections (approximately 100 nm) were cut with a diamond knife and stained with uranyl acetate and lead citrate on grids. Stained sections were observed with TEM.

### 4.4 | Effect of active 5-FU derivatives on clinical strains

The compounds that showed considerable activity against both Gram-negative and Gram-positive bacteria were tested further on clinically isolated strains. The test was carried out similarly as mentioned in the susceptibility experiment given in Section 4.2.

### 4.5 | Membrane permeabilization assays

#### 4.5.1 | Membrane perturbation in Gram-positive bacteria using the PI assay

*S. aureus* (SA-1199) was grown to the mid-log phase and adjusted to OD<sub>600</sub> 0.3 in MH-II medium. The prepared bacterial suspension (1 mL) was then mixed with 1 mL of PI solution (10 µg/mL). An aliquot (50 µL) of PI-mixed bacterial suspension was added to each well in a 96-well plate. Subsequently, 50 µL of twofold of desired concentration of **6c** was added to the PI-mixed bacterial suspension and incubated with gentle shaking for 30 min. PI fluorescence was measured at excitation and emission wavelengths of 580 and 620 nm, respectively. Cells treated with PBS and Triton X-100 (1% w/v) served as a negative as a positive control.

#### 4.5.2 | Membrane perturbation in Gram-negative bacteria using nitrocefin assay

The ability of the most active **6c** to permeabilize the outer membrane of bacteria was estimated using a colourimetric nitrocefin hydrolysis assay.<sup>[69]</sup> Nitrocefin is a chromogenic cephalosporin that changes colour when hydrolysed by periplasmic β-lactamases from yellow to red. For this

assay, fresh bacterial suspension (OD<sub>600</sub> 0.5) of EA289 and T-AG100 was prepared in potassium phosphate buffer (PPB, pH 7.4) containing MgCl<sub>2</sub> (1 mM). An aliquot (100 µL) of the prepared cell suspension was then transferred to each well of the flat-bottomed, 96-well microplate (Corning™ CoStar™) followed by 50 µL of **6c** test solutions (fourfold the desired concentration). Similarly, 50 µL of PMB solution (32–0.25 µg/mL) and PPB buffer, pH 7.4 were added separately to other wells to serve as positive and negative controls, respectively. An aliquot (50 µL) of nitrocefin solution was added to each well just before reading the microplate, and the absorbance was measured in a microplate reader (Tecan, Infinite M200 Pro) at 490 nm every 1 min for 60 min.

#### 4.6 | Motility assay

Motility is the most impressive ability of bacteria, which aids its translocation to preferred hosts and access to optimal colonization sites within them. Tests were performed to evaluate the ability of **6c** to suppress motility functions in bacteria. For this assay, *P. aeruginosa* PAO1 was grown on 1.5% w/v Luria-Bertani (LB) agar and suspended in LB broth just before the experiment to achieve a cell density of OD<sub>600</sub> 0.1.

##### 4.6.1 | Swimming

Swim plates were prepared using media consisting of tryptone (10 g/L), NaCl (5 g/L) and agarose (3 g/L). Inoculation of cell suspension was carried out by gently touching a single spot at the centre of the plate using a sterile toothpick. The plates were then incubated at 30°C for 12–14 h.<sup>[33]</sup>

##### 4.6.2 | Swarming

Swarming plates were prepared using media consisting of bactoagar (5 g/L), nutrient broth (8 g/L) and glucose (5 g/L). Swarm plates were typically allowed to dry at room temperature overnight before being used. Inoculation and incubation were carried out in the same way as with swim plates.<sup>[33]</sup>

##### 4.6.3 | Twitching

Twitch plates were prepared using tryptone (10 g/L), yeast extract (5 g/L), NaCl (10 g/L) and granulated agar (10 g/L). Plates were dried and stabbed using a sterile toothpick with the inoculum perpendicular to the agar down to the agar-plastic interface. Plates were then incubated in a humidified environment at 37°C for 24 h. The following day, plates were flooded with TM developer solution. After 30 min, the plates were decanted, and the opaque white halo obtained at the bottom of the plates was observed and measured.<sup>[70]</sup>

#### 4.7 | Haemolytic activity

Residual human blood was procured from HIA-Laveran. The RBCs were separated from plasma by centrifugation at 2000 rpm for 10 min, washed and resuspended in PBS (pH 7.4). A stock solution of **6c** was prepared in DMSO (20 mg/mL) and diluted with PBS to yield 100-fold the desired concentration (10–100 µg/mL). Further, 10 µL of each concentration was added separately to centrifuge tubes containing 490 µL of PBS (pH 7.4) and 500 µL of RBC dispersion. Concurrently, RBC dispersion was treated separately with PBS (pH 7.4) and Triton X-100 (final concentration: 1% w/v) were used as negative and positive controls, respectively. All the tubes were incubated for 30 min at 37°C and later centrifuged at 2000 rpm for 10 min. The supernatants thus obtained (400 µL) were transferred to spectrometric cuvettes, and a Cobas 6000 analyser (Hitachi) was used to calculate the percentage haemoglobin release at 550 nm. The following Equation (1) was used to calculate the percentage of haemolysis:

$$\begin{aligned} \% \text{ Haemolysis} &= \frac{(\text{Absorbance of test} - \text{Absorbance of negative control})}{(\text{Absorbance of positive control} - \text{Absorbance of negative control})} \quad (1) \\ &\times 100. \end{aligned}$$

As per Amin et al., a haemolysis value above 25% was deemed to be haemolytic.<sup>[71]</sup>

#### 4.8 | Statistical analysis

Graphs were plotted using GraphPad Prism 6 (GraphPad Inc.). Data were analysed using the student *t*-test analysis for differences between the two groups, and findings were expressed as means ± SD. For more than one group one-way analysis of variance, followed by Tukey's multiple comparisons was used. All assays included three replicates and were repeated in at least three independent experiments. A *p* < 0.05 was considered to be statistically significant. \**p* < 0.05; \*\**p* < 0.01; \*\*\**p* < 0.001; \*\*\*\**p* < 0.0001.

#### ACKNOWLEDGEMENTS

Pr. Eric Garnotel and Dr. Hélène Astier (HIA Laveran-Marseille) are deeply acknowledged for providing us with clinical isolates and technical advice. We are thankful to Dr. Veronique Sinou (MCT, AMU, Marseille) and Dr. Lorena Tuchscher (Institute of Medical Microbiology, Jena University Hospital, Germany) for providing ESKAPE reference bacteria and SAK1758 bacteria, respectively. We thank Agnès Chambard for helping during her internship in the synthesis of a chemical intermediate. This work was supported in part by Inserm, Aix-Marseille University, CNRS and MESRI (Ministère de l'Enseignement Supérieur de la Recherche et de l'Innovation). Main fundings were obtained by Amidex Foundation grant no. A-M-AAP-ID-17-22-170228-18.54. Open access funding provided by COUPERIN CY23 - Aix-Marseille Université.

## CONFLICT OF INTEREST STATEMENT

The authors declare no conflicts of interest.

## ORCID

Krykun Serhii  <http://orcid.org/0000-0001-8818-0154>

Suzanne Giorgio  <http://orcid.org/0000-0003-3400-896X>

Michel Camplo  <http://orcid.org/0000-0002-4446-0661>

## REFERENCES

- [1] L. S. J. Roope, R. D. Smith, K. B. Pouwels, J. Buchanan, L. Abel, P. Eibich, C. C. Butler, P. S. Tan, A. S. Walker, J. V. Robotham, S. Wordsworth, *Science* **2019**, *364*, 1.
- [2] L. B. Rice, *J. Infect. Dis.* **2008**, *197*, 1079.
- [3] J. O'Neill, *Tackling Drug-Resistant Infections Globally: Final Report and Recommendations*. Wellcome trust, HM Government **2016**.
- [4] World Health Organization, *Cad. Pesqui.* **2017**, *43*.
- [5] R. Laxminarayan, A. Duse, C. Watal, A. K. M. Zaidi, H. F. L. Wertheim, N. Sumpradit, E. Vlieghe, G. L. Hara, I. M. Gould, H. Goossens, C. Greko, A. D. So, M. Bigdeli, G. Tomson, W. Woodhouse, E. Ombaka, A. Q. Peralta, F. N. Qamar, F. Mir, S. Kariuki, Z. A. Bhutta, A. Coates, R. Bergstrom, G. D. Wright, E. D. Brown, O. Cars, *Lancet Infect. Dis.* **2013**, *13*, 1057.
- [6] J. G. Bartlett, D. N. Gilbert, B. Spellberg, *Clin. Infect. Dis.* **2013**, *56*, 1445.
- [7] L. J. Piddock, *Lancet Infect. Dis.* **2012**, *12*, 249.
- [8] O. B. Jonas, A. Irwin, F. C. J. Berthe, F. G. Le Gall, P. V. Marquez, *Drug-Resistant Infections: A Threat to Our Economic Future (Discussion Draft)*, International Bank For Reconstruction and Development, Washington DC, USA **2017**. [www.worldbank.org](http://www.worldbank.org)
- [9] A. Chokshi, Z. Sifri, D. Cennimo, H. Horng, *J. Glob. Infect. Dis.* **2019**, *11*, 36.
- [10] M. A. Farha, E. D. Brown, *Nat. Microbiol.* **2019**, *4*, 565.
- [11] B. M. Sahoo, B. V. V. Ravi Kumar, J. Sruti, M. K. Mahapatra, B. K. Banik, P. Borah, *Front. Mol. Biosci.* **2021**, *8*, 1.
- [12] A. E. J. Yssel, J. Vanderleyden, H. P. Steenackers, *J. Antimicrob. Chemother.* **2017**, *72*, 2156.
- [13] S. S. Cohen, J. G. Flaks, H. D. Barner, M. R. Loeb, J. Lichtenstein, *Proc. Natl. Acad. Sci. USA* **1958**, *44*, 1004.
- [14] A. Tomasz, E. Borek, *Proc. Natl. Acad. Sci. USA* **1960**, *46*, 324.
- [15] F. Sedlmayer, A. Woischnig, V. Unterreiner, F. Fuchs, D. Baeschlin, N. Khanna, M. Fussenegger, *Nucleic Acids Res.* **2021**, *49*, 1.
- [16] A. Ueda, C. Attila, M. Whiteley, T. K. Wood, *Microb. Biotechnol.* **2009**, *2*, 62.
- [17] M. Hussain, C. Collins, J. G. M. Hastings, P. J. White, *J. Med. Microbiol.* **1992**, *37*, 62.
- [18] X. L. Dai, A. P. Voronin, W. Gao, G. L. Perlovich, T. B. Lu, J. M. Chen, *CrystEngComm* **2019**, *21*, 5095.
- [19] C. Pfab, A. Abgaryan, B. Danzer, F. Mourtada, W. Ali, A. Gessner, N. El-Najjar, *BMC Cancer* **2022**, *22*, 125.
- [20] F. Brunel, C. Lautard, C. di Giorgio, F. Garzino, J. M. Raimundo, J. M. Bolla, M. Camplo, *Bioorg. Med. Chem. Lett.* **2018**, *28*, 926.
- [21] F. Brunel, C. Lautard, F. Garzino, S. Giorgio, J. M. Raimundo, J. M. Bolla, M. Camplo, *Bioorg. Med. Chem. Lett.* **2016**, *26*, 3770.
- [22] F. Brunel, C. Lautard, F. Garzino, J. M. Raimundo, J. M. Bolla, M. Camplo, *Bioorg. Med. Chem. Lett.* **2020**, *30*, 127389.
- [23] S. Carrara, F. Rouvier, S. Auditto, F. Brunel, C. Jeanneau, M. Camplo, M. Sergent, I. About, J. M. Bolla, J. M. Raimundo, *Int. J. Mol. Sci.* **2022**, *23*, 2183.
- [24] Y. C. Yeh, T. H. Huang, S. C. Yang, C. C. Chen, J. Y. Fang, *Front. Chem.* **2020**, *8*, 286.
- [25] S. Zimmermann, M. Klinger-Strobel, J. A. Bohnert, S. Wendler, J. Rödel, M. W. Pletz, B. Löffler, L. Tuchscher, *Front. Microbiol.* **2019**, *10*, 1.
- [26] S. Zimmermann, L. Tuchscher, J. Rödel, B. Löffler, J. A. Bohnert, *J. Microbiol. Methods* **2017**, *142*, 39.
- [27] V. Kuete, B. Ngameni, J. G. Tangmouo, J. M. Bolla, S. Alibert-Franco, B. T. Ngadjui, J. M. Pagès, *Antimicrob. Agents Chemother.* **2010**, *54*, 1749.
- [28] J. Vergalli, A. Atzori, J. Pajovic, E. Dumont, G. Mallocci, M. Masi, A. V. Vargiu, M. Winterhalter, M. Réfrégiers, P. Ruggerone, J. M. Pagès, *Commun. Biol.* **2020**, *3*, 198.
- [29] M. H. Mustafa, H. Chalhoub, O. Denis, A. Deplano, A. Vergison, H. Rodriguez-Villalobos, M. M. Tunney, J. S. Elborn, B. C. Kahl, H. Traore, F. Vanderbist, P. M. Tulkens, F. Van Bambeke, *Antimicrob. Agents Chemother.* **2016**, *60*, 6735.
- [30] H. Chalhoub, Y. Sáenz, W. W. Nichols, P. M. Tulkens, F. Van Bambeke, *Int. J. Antimicrob. Agents* **2018**, *52*, 697.
- [31] M. A. Jacobs, A. Alwood, I. Thaipisuttikul, D. Spencer, E. Haugen, S. Ernst, O. Will, R. Kaul, C. Raymond, R. Levy, L. Chun-Rong, D. Guenther, D. Bovee, M. V. Olson, C. Manoel, *Proc. Natl. Acad. Sci. USA* **2003**, *100*, 14339.
- [32] A. Troudi, H. Douafer, J.-M. Bolla, N. Klibi, J. M. Brunel, *Antiinfect. Agents* **2021**, *19*, 110.
- [33] D. Borselli, A. Lieutaud, H. Thefenne, E. Garnotel, J. M. Pagès, J. M. Brunel, J. M. Bolla, *PLoS One* **2016**, *11*, 1.
- [34] J. M. Pages, J. P. Lavigne, V. Leflon-Guibout, E. Marcon, F. Bert, L. Noussair, M. H. Nicolas-Chanoine, *PLoS One* **2009**, *4*, e4817.
- [35] R. D. Magnini, A. Hilou, H. Millogo-Koné, J. M. Pagès, A. Davin-Regli, *Antibiotics* **2020**, *9*, 323.
- [36] A. V. Vargiu, H. Nikaido, *Proc. Natl. Acad. Sci. USA* **2012**, *109*, 20637.
- [37] R. C. Oliver, J. Lipfert, D. A. Fox, R. H. Lo, S. Doniach, L. Columbus, *PLoS One* **2013**, *8*, e62488.
- [38] R. F. Matias, T. J. Beveridge, *J. Bacteriol.* **2006**, *188*, 1011.
- [39] A. Zajmi, N. Mohd Hashim, M. I. Noordin, S. A. M. Khalifa, F. Ramli, H. Mohd Ali, H. R. El-Seedi, *PLoS One* **2015**, *10*, 1.
- [40] A. Grigor'eva, A. Bardasheva, A. Tupitsyna, N. Amirkanov, N. Tikunova, D. Pyshnyi, E. Ryabchikova, *Microorganisms* **2020**, *8*, 1.
- [41] H. Adler, E. M. Schraner, R. Frei, P. Wild, *Microsc. Microanal.* **2005**, *11*, 982.
- [42] M. Nega, P. M. Tribelli, K. Hipp, M. Stahl, F. Götz, *Commun. Biol.* **2020**, *3*, 695.
- [43] M. A. Azad, H. E. K. Huttunen-Hennelly, C. Ross Friedman, *Antimicrob. Agents Chemother.* **2011**, *55*, 2137.
- [44] C. Jensen, H. Li, M. Vestergaard, A. Dalsgaard, D. Frees, J. J. Leisner, *Front. Microbiol.* **2020**, *11*, 1.
- [45] L. Santhana Raj, H. L. Hing, O. Baharudin, Z. Teh Hamidah, R. Aida Suhana, C. P. Nor Asih, B. Vimala, S. Paramsarvaran, G. Sumarni, K. Hanjeet, *Trop. Biomed.* **2007**, *24*, 105.
- [46] M. Hartmann, M. Berditsch, J. Hawecker, M. F. Ardakani, D. Gerthsen, A. S. Ulrich, *Antimicrob. Agents Chemother.* **2010**, *54*, 3132.
- [47] D. Morita, H. Sawada, W. Ogawa, H. Miyachi, T. Kuroda, *Biochim. Biophys. Acta—Biomembr.* **2015**, *1848*, 2057.
- [48] M. Shimoda, K. Ohki, Y. Shimamoto, O. Kohashi, *Infect. Immun.* **1995**, *63*, 2886.
- [49] A. Grigor'eva, I. Saranina, N. Tikunova, A. Safonov, N. Timoshenko, A. Rebrov, E. Ryabchikova, *Biometals* **2013**, *26*, 479.
- [50] R. A. Weigand, J. M. Shively, J. W. Greenawalt, *J. Bacteriol.* **1970**, *102*, 240.
- [51] A. Oliveira, H. G. Ribeiro, A. C. Silva, M. D. Silva, J. C. Sousa, C. F. Rodrigues, L. D. R. Melo, A. F. Henriques, S. Sillankorva, *Front. Microbiol.* **2017**, *8*, 2407.
- [52] I. M. Famuyide, F. O. Fasina, J. N. Eloff, L. J. McGaw, *BMC Vet. Res.* **2020**, *16*, 326.
- [53] H. Schwarz, A. L. Koch, *Microbiology* **1995**, *141*, 3161.
- [54] B. Alkotaini, N. Anuar, A. A. H. Kadhum, *Appl. Biochem. Biotechnol.* **2015**, *175*, 1868.

- [55] L. Li, C. Shi, Z. Yin, R. Jia, L. Peng, S. Kang, Z. Li, *Braz. J. Microbiol.* **2014**, *45*, 1409.
- [56] J. Y. Kim, C. Lee, M. Cho, J. Yoon, *Water Res.* **2008**, *42*, 356.
- [57] S. U. Vetterli, K. Zerbe, M. Müller, M. Urfer, M. Mondal, S. Y. Wang, K. Moehle, O. Zerbe, A. Vitale, G. Pessi, L. Eberl, B. Wollscheid, J. A. Robinson, *Sci. Adv.* **2018**, *4*, 2634.
- [58] J. H. Gieringer, A. F. Wenz, H. M. Just, F. D. Daschner, *Chemotherapy* **1986**, *32*, 418.
- [59] D. Borselli, M. Blanchet, J. M. Bolla, A. Muth, K. Skruber, O. Phanstiel, J. M. Brunel, *ChemBioChem* **2017**, *18*, 276. <https://doi.org/10.1002/cbic.201600532>
- [60] J. M. Benarroch, M. Asally, *Trends Microbiol.* **2020**, *28*, 304.
- [61] C. O'May, N. Tufenkji, *Appl. Environ. Microbiol.* **2011**, *77*, 2677.
- [62] K. Dimmitt, S. Bradford, M. Simon, *J. Bacteriol.* **1968**, *95*, 801.
- [63] S. J. Kerr, *J. Gen. Microbiol.* **1972**, *72*, 419.
- [64] A. A. Niazy, R. N. A. Lambarte, H. S. Alghamdi, *J. King Saud Univ. Sci.* **2022**, *34*, 102040.
- [65] C. Attila, A. Ueda, T. K. Wood, *Appl. Microbiol. Biotechnol.* **2009**, *82*, 525.
- [66] T. P. West, *Microbiol. Res.* **2014**, *169*, 954.
- [67] Clinical and Laboratory Standards Institute (CLSI) Guidelines. *Methods for Dilution Antimicrobial Susceptibility Tests for Bacteria That Grow Aerobically; Approved Standard*, 9th ed. Wayne, Pennsylvania, USA **2012**.
- [68] D. Ghisalberti, M. Masi, J. M. Pagès, J. Chevalier, *Biochem. Biophys. Res. Commun.* **2005**, *328*, 1113.
- [69] A. Lieutaud, E. Guinoiseau, V. Lorenzi, M. C. Giuliani, V. Lome, J.-M. Brunel, A. Luciani, J. Casanova, J.-M. Pages, L. Berti, J. M. Bolla, *Antimicrob. Agents* **2013**, *11*, 168.
- [70] Lynne Turnbull, B. Cynthia. *Whitchurch*, in (Eds: Alain Filloux, Juan-Luis Ramos), Springer Science+Business Media, New York. **2014**.
- [71] K. Amin, R. M. Dannenfels, *J. Pharm. Sci.* **2006**, *95*, 1173.

## SUPPORTING INFORMATION

Additional supporting information can be found online in the Supporting Information section at the end of this article.

**How to cite this article:** M. Patil, K. Serhii, F. Garzino, Q. Gobert, S. Giorgio, J.-M. Raimundo, J.-M. Bolla, M. Camplo, *Arch. Pharm.* **2023**, e2300103.  
<https://doi.org/10.1002/ardp.202300103>